

## Earthquake Swarms on the Mid-Atlantic Ridge: Products of Magmatism or Extensional Tectonics?

ERIC A. BERGMAN AND SEAN C. SOLOMON

*Department of Earth, Atmospheric, and Planetary Sciences, Massachusetts Institute of Technology, Cambridge*

By analogy with the microearthquake swarms which accompany terrestrial volcanic eruptions, teleseismically observed earthquake swarms along mid-ocean ridges are commonly thought to be indicators of volcanism, particularly dike emplacement. We test this assumption by investigating the spatial and temporal patterns and other characteristics of earthquakes in 34 swarms on the Mid-Atlantic Ridge. Resolution of the relative locations of swarm events is improved by the use of a multiple-event relocation technique. Most swarms extend 5 to 15 km across the ridge axis and 5 to 20 km along it. None of the swarms displays the large length-to-width ratio and temporal migration of epicenters along axis which are characteristic of earthquake swarms in the well-studied rift zones of Hawaii and Iceland. The relative locations, magnitudes, and source mechanisms of swarm events are most easily explained if teleseismically observable swarms are expressions of extension across a substantial portion of the median valley and perhaps into the rift mountains. The possibility that some of these swarms include events directly associated with magmatic intrusion cannot be excluded, however. Like their terrestrial counterparts, purely volcanic earthquakes on the mid-ocean ridges probably occur dominantly at magnitudes below the teleseismic detection threshold of global seismic networks ( $m_b < 4.5$ ). The largest normal-faulting earthquakes on mid-ocean ridges and many of the teleseismically observed swarms likely occur on the faults marking the inner rift wall, where the crust first experiences significant faulting and is broken into numerous closely-spaced normal faults. We speculate that the high degree of order in the dimensions, spacing, throws, and mechanical properties of these faults, combined with stress concentrations arising naturally from the mechanical behavior of the lithosphere at rifted, slow-spreading ridges, may account for the common occurrence of earthquake swarms.

### INTRODUCTION

Earthquake swarms are commonly, but not exclusively, associated with volcanism. Sykes [1970] noted that swarms of teleseismically located earthquakes occur frequently on segments of the mid-ocean ridge system, and he postulated a close relationship between such seismicity and the magmatic processes involved in plate creation. Subsequent research on earthquake swarms on mid-ocean ridges has focussed on observations of microearthquake swarms with networks of ocean bottom seismometers [Francis *et al.*, 1978; Lilwall *et al.*, 1978; Brocher, 1983] or floating sonobuoys [e.g., Reichle and Reid, 1977] and teleseismic source studies of the largest swarm events [e.g., Thatcher and Brune, 1971; Tatham and Savino, 1974; Huang *et al.*, 1986]. Opportunities for both types of study are rare. Swarm events in the magnitude range between microearthquakes and the largest ridge axis earthquakes have received little attention. Partly because of the scarcity of detailed observations, our understanding of the significance of mid-ocean ridge earthquake swarms has improved little in two decades, and the possibility that swarm earthquakes signal active volcanism on the accretionary axis remains a frequent suggestion [e.g., Lilwall, 1982]. In this paper we address the causes of earthquake swarms on mid-ocean ridges by means of a detailed study of the spatial and temporal patterns of teleseismically detected swarms on the northern Mid-Atlantic Ridge.

Earthquakes on mid-ocean ridges can, in principle, be grouped into two classes, according to their association with the two primary phases of the spreading cycle of slow-spreading ridges: (1) creation of new oceanic crust by the

intrusion of crustal dike systems from shallow axial magma chambers and eruption of material onto the seafloor [e.g., Cann, 1970; Aumento *et al.*, 1971; Lewis, 1983], and (2) extensional tectonism as the newly created crust is accelerated to full spreading velocity, faulted, and uplifted to yield the topographic relief of the rift mountains [e.g., Harrison, 1974; Harrison and Stieltjes, 1977; Macdonald and Atwater, 1978]. This distinction is similar to the classification of earthquakes at Kilauea volcano as “rift” events, which accompany episodes of magmatic intrusion or eruption, and “flank” events, which represent the response of the surrounding crust to the stresses introduced during intrusion [Klein, 1982]. A large earthquake swarm in the Galapagos Islands in June 1968 may represent an exception to this classification; Francis [1974] proposed that the swarm resulted from the collapse of the Fernandina caldera following the withdrawal of magma from shallow crustal levels. Whether or not an axial magma chamber is commonplace beneath slow-spreading ridges [e.g., Macdonald, 1982; Stakes *et al.*, 1984], episodes of eruptive activity are probably relatively short-lived and infrequent [e.g., Hall, 1976]. In this context, the observation that virtually the entire Mid-Atlantic Ridge (MAR) is seismically active at time periods greater than a few years [Einarsson, 1979] and that a large fraction of this seismicity occurs as swarms [Francis and Porter, 1971] leads one to expect that most teleseismic swarms on the MAR are likely to represent extensional tectonic processes. Even if this line of reasoning is accepted, however, the question remains as to whether there exists a distinguishable subset of swarms which is associated with active eruption events.

The most widely-applied class of models linking earthquake swarms with active volcanism focusses on the role of

Copyright 1990 by the American Geophysical Union.

Paper number 89JB03451.  
0148-0227/90/89JB-03451\$05.00

dike emplacement. Hill [1977] proposed a quantitative model attributing earthquake swarms to shear failure on conjugate faults between the tips of an echelon magma-filled dikes. Shaw [1980] modified this model to include the possibility that the shear fractures connecting dike tips might act as magma conduits between dike segments. Levelling data in Iceland have been interpreted to indicate that a major fraction of slip occurs on relatively deep faults in advance of the propagating dike [Rubin and Pollard, 1988]. This deformation could contribute a second population of earthquakes to swarms. For both the Hill and the Rubin-Pollard models, a tendency for the earthquake swarm to track the moving front of the magma intrusion is predicted.

Another mechanism by which dike intrusion may produce earthquakes has been suggested by source studies of several large ( $M_s \sim 6$ ) events in a 1980 swarm near Long Valley caldera, in eastern California [Julian, 1983]. Seismological evidence strongly supports the hypothesis that these earthquakes were the result of tensile failure under high fluid pressure [Julian and Sipkin, 1985]. Tensile cracking mechanisms for microearthquakes in Iceland have been reported [Foulger and Long, 1984], but the large size of the Long Valley earthquakes appears to be unusual. The rarity of such events, combined with the continental tectonic setting and the silicic nature of the volcanism there, prevent us from taking this example as a likely analog to the seismotectonics of the mid-ocean ridge system, but we cannot dismiss the possibility that fluid-driven tensile failure may account for some teleseismically observed mid-ocean ridge earthquakes.

The segmentation of the mid-ocean ridge system places constraints on the organization of the magmatic system which supplies individual spreading segments [Whitehead *et al.*, 1984; Schouten *et al.*, 1985]. Current models for the accretion process at slow-spreading ridges suggest that persistent axial magma chambers are unlikely to exist at more than one or two sites along an active ridge segment, implying that significant episodes of lateral magma intrusion over distances of tens of kilometers may occur during an eruptive episode [e.g., Macdonald, 1986]. It is reasonable to suppose that such lateral migration is accomplished through propagating dike swarms contained within a relatively narrow rift zone along the inner floor of the median valley and that such episodes are accompanied by swarms of small earthquakes, in close analogy to the observations in the active rift zones of Iceland and other terrestrial volcanic centers.

We thus pose the hypothesis that at least some teleseismically observed earthquake swarms represent such an episode of dike propagation and therefore reveal the presence of magma. If this hypothesis were shown to be generally correct, teleseismic data could be used to place constraints on the geometry of the magma supply system to individual spreading cells and guide the planning of detailed investigations of magmatic systems, for example with ocean-bottom seismometer networks and submersibles. We test this hypothesis by comparing teleseismically-observable characteristics, in particular the spatial and temporal patterns, of mid-ocean ridge earthquake swarms with those of well-studied earthquake swarms associated with lateral magma migration. Improved resolution of these patterns for the mid-ocean ridge events is achieved by a multiple-event relocation technique.

#### EARTHQUAKE SWARMS AND DIKE EMPLACEMENT IN TERRESTRIAL RIFT ZONES

The detailed observations needed to reveal relationships between magmatic activity and earthquake swarms are available only for a few terrestrial sites of basaltic volcanism (notably Iceland, Hawaii, and the Afar), none of which can be taken as a completely satisfactory analog to a normal oceanic spreading segment. Hawaii, of course, is in an intraplate setting, with a regional stress field quite different from the extensional stress regime of the mid-ocean ridges. While Iceland is part of the Mid-Atlantic Ridge, like Hawaii it is a hotspot. The Ghoubbet-Asal Rift in the Afar is more similar to a mid-ocean ridge than Iceland [Needham *et al.*, 1976; Tamsett, 1986], but it is a very immature spreading system, still dominated by the pre-existing structure of the continental crust. If these distinctions are kept in mind, however, the terrestrial observations are still useful in evaluating the significance of the limited teleseismic observations available for the study of earthquake swarms on mid-ocean ridges.

#### Iceland

While Iceland is atypical of the mid-ocean ridge system, many of the processes of accretionary tectonics which can be closely observed there are likely to be good analogs to the processes occurring along the submerged portions of the ridge [e.g., Tryggvason, 1973]. Migration of swarm seismicity was observed on the Reykjanes Peninsula in 1972, in a rift zone approximately 2 km wide and 12 km in length, but no direct evidence of magma flow was found [Klein *et al.*, 1977]. Such a link between swarm activity and magma transport has been established, however, at the Krafla volcano in northern Iceland. During a major rifting episode lasting from 1975 to 1984, the volcano inflated and deflated as many as 20 times [Björnsson *et al.*, 1977; Wendt *et al.*, 1985]. Inflation occurred during replenishment of the shallow magma body beneath the central caldera. The deflation events involved injection of magma laterally into fissure swarms north and south of the caldera, accompanied by earthquake swarms which often tracked the position of the magma front [Brandsdóttir and Einarsson, 1979; Einarsson and Brandsdóttir, 1980]. The active rift zones were 5 km or less in width and had a total length of 80 km. In the July 1978 deflation event, the rate of migration of the earthquake swarm reached  $1.8 \text{ km h}^{-1}$  during the first nine hours [Einarsson and Brandsdóttir, 1980].

Only two of the deflationary events were accompanied by a significant number of earthquakes sufficiently large to be well-recorded at teleseismic distances. The first episode of such activity began several days after the initiation of rifting, on December 24, 1975, and lasted until early February 1976. The earthquakes were concentrated spatially in two clusters, one near Krafla caldera, the second 40–60 km north of the caldera, at the intersection of the rift zone with the Tjörnes Fracture Zone [Ward, 1971; Einarsson and Brandsdóttir, 1980]. Although much of this seismicity must have been associated with the extensive surface fracturing and rifting which occurred simultaneously [Sigurdsson, 1980], the largest earthquake in the swarm ( $m_b = 5.9$ ) was found by Einarsson [1979] to have a strike-slip focal mechanism consistent with transform motion on the fracture zone. During a second deflationary event, in January 1978, earth-

quakes were again concentrated in the fissure swarm north of the caldera, immediately to the south of the source region of the 1975–1976 earthquake swarm. These two swarms each resulted in about 1 m of subsidence in a graben approximately 5 km wide and 20 km long [Sigurdsson, 1980].

### Hawaii

The association of earthquake swarms with episodes of lateral magma intrusion into the rift zones of Kilauea and Mauna Loa volcanoes has been well-documented by many years of detailed observations [Klein *et al.*, 1987], and swarms have also been detected at the recently formed Loihi submarine volcano southeast of Hawaii [Klein, 1982]. Swarms are particularly common in the early stages of an eruptive event. At the mature rift zones of Kilauea and Mauna Loa, earthquake swarms generally last only a few days, but several swarms lasting several months have been observed at Loihi. Migration usually occurs down-rift from the summit caldera, at rates of 0.1 to 6 km h<sup>-1</sup>. Concentrations of earthquakes are thought to occur at barriers within the conduit system, arising from geometrical constraints or stress concentrations, and these points frequently serve as initiation or stopping points for intrusive episodes. Intrusive events tend to be clustered in pairs or triples over the course of several weeks, alternating between several rift zones. The largest earthquakes directly associated with dike intrusion events have local magnitudes of about 4.0. In a detailed study of four swarms Karpin and Thurber [1987] found that most of the earthquakes have strike-slip mechanisms, in agreement with the model of Hill [1977].

### Afar

The tectonics of the Afar region, including Djibouti, are dominated by the propagation of a spreading center into the continental crust of Africa as part of a ridge-ridge-ridge triple junction whose other arms are young oceanic spreading centers in the Gulf of Aden and Red Sea [Mohr, 1970]. With the conspicuous exception that it is not presently covered by water, portions of the Afar resemble in many ways a typical segment of the Mid-Atlantic Ridge [Needham *et al.*, 1976; Tamsett, 1986]. A major earthquake swarm occurred within the Ghoubbet-Asal Rift in November and December 1978. The largest event ( $m_b = 5.3$ ) occurred on the second day of the swarm at the southeastern end of the subaerial section of the rift. Most of the seismicity, including many events with  $m_b > 4.0$ , occurred to the southeast of this epicenter, beneath the Ghoubbet al Kharab [Abdallah *et al.*, 1979]. The focal mechanisms of these events indicate normal faulting on faults parallel to the rift axis. At the time of the swarm, faults and fissures were created or reactivated over a zone 3–4 km wide along the full length of the subaerial part of the rift (15 km). Including the seismically active portion beneath Ghoubbet al Kharab, the length of the rift which was active during this rifting episode totals 30 km. At the northwestern end of the subaerial portion of the rift, near Lake Asal, a basaltic fissure eruption began shortly after the largest earthquake and continued for a week [Allard *et al.*, 1979]. Ruegg *et al.* [1979] concluded that magmatism played a small role in the rifting event, which was dominated by the brittle failure and elastic rebound of the lithosphere along the rift.

## TELESEISMICALLY LOCATED SWARMS ON THE NORTHERN MID-ATLANTIC RIDGE

### Earthquake Data Set

The northern Mid-Atlantic Ridge was chosen for this study because the distribution of seismic stations at teleseismic distances is good, because the tectonics of this ridge system are relatively well-understood, and because of the proximity to Iceland, the best terrestrial example of the association between earthquake swarms and lateral magma migration during active rifting. We searched the catalog of the International Seismological Centre (ISC) for earthquakes on the MAR between 10°N (Vema Fracture Zone) and 60°N (immediately south of Iceland) in the years 1964–1985 having at least 10 teleseismic (epicentral distance  $\Delta > 25^\circ$ ) arrival times. In the northern part of the study region, particularly the Reykjanes Ridge, events which have very few teleseismic data can often be located because of the proximity of seismic stations in Iceland and Europe; comparable earthquakes farther south may escape detection. The criterion on number of teleseismic arrivals in the catalog search maintains a reasonably consistent sampling procedure over the study area. Groups of three or more earthquakes clustered in space (<50 km) and time (<1 week) were included in the initial list of earthquake swarms. The time window considered was expanded to several weeks for a few swarms containing many events. Events on large-offset transform faults were removed, as were obvious mainshock-aftershock sequences, but several swarms retained for this study include earthquakes as large ( $m_b > 5.5$ ) as any that occur on the spreading ridge segments of the MAR. We retained only swarms containing at least three events which could be relocated with good confidence (as discussed below). Swarms with fewer than five events were retained only if they were close enough to other swarms to allow simultaneous relocation of the entire group, since the benefits of simultaneous relocation increase with the number of earthquakes included.

Beginning on May 21, 1989, an unusually intense swarm near 60°N on the Reykjanes Ridge attracted considerable interest in the geophysical community because of the possibility that it might signal an episode of active volcanism (R. Holcomb, pers. comm., 1989). The last of the 46 events in the series located by the National Earthquake Information Service (NEIS) occurred on June 11. An airborne deployment of a sonobuoy network was made on June 13, at which time the level of microearthquake activity was still quite high (C. Nishimura, personal communication, 1989). Bathymetric and water column measurements in the area of the swarm were made by the research vessels Atlantis II and Endeavor in June (J. Delaney, personal communication, 1989).

Because of the widespread interest in this swarm we have included it in the study, but because of its recency the procedures differed slightly from those followed for the remaining swarms. The arrival time data were obtained from the NEIS Preliminary Determination of Epicenters (PDE). We attempted to relocate all events listed in the PDE, even those with fewer than 10 teleseismic arrival times. Nine events could not be relocated with acceptable confidence, however, and these were eliminated. Finally, we made use of arrival times from the Icelandic stations REY ( $\Delta \sim 6^\circ$ ) and AKU ( $\Delta \sim 8^\circ$ ), because otherwise station coverage was too sparse for many of the smaller events to be located.

TABLE 1. Teleseismically Relocated Swarms

Date	Epicentroid <sup>a</sup>		N <sup>b</sup>	L <sup>c</sup>	W <sup>d</sup>	Pointlike <sup>e</sup>	Figure
	Latitude, °N	Longitude, °W					
June 10, 1971	59.45 ± 0.016	30.35 ± 0.021	4	12 ± 4	11 ± 3	no	6
April 11, 1977	59.45	30.16	4	18 ± 5	3 ± 3	no	
Jan. 18, 1983	59.38	30.34	3	3 ± 4	11 ± 2	yes	
May 21, 1989	59.87	29.69	37	37 ± 5	21 ± 3	no	
Nov. 3, 1965	58.18 ± 0.013	32.14 ± 0.012	3	12 ± 9	10 ± 6	yes	7
Sept. 20, 1969	58.19	32.13	6	12 ± 3	15 ± 2	no	
Feb. 17, 1983	58.55	31.61	14	37 ± 4	28 ± 3	no	
Sept. 28, 1970	57.18 ± 0.014	33.31 ± 0.013	3	5 ± 4	6 ± 2	yes	8
Jan. 26, 1977	57.64	33.00	3	13 ± 7	8 ± 3	yes	
Aug. 3, 1984	57.65	32.84	5	7 ± 3	15 ± 2	no	
March 9, 1967	56.02 ± 0.015	34.67 ± 0.016	17	44 ± 7	10 ± 4	no	9
April 23, 1970	55.52	35.08	7	23 ± 5	16 ± 4	no	
Sept. 25, 1965	54.03 ± 0.016	35.27 ± 0.011	3	3 ± 13	7 ± 5	yes	10
April 3, 1972	54.27	35.11	3	6 ± 2	7 ± 4	yes <sup>f</sup>	
March 23, 1974	53.89	35.46	3	4 ± 5	9 ± 2	yes	
July 31, 1984	53.98	35.14	3	13 ± 4	2 ± 2	no	
Nov. 10, 1967	45.03 ± 0.017	28.10 ± 0.010	3	19 ± 9	11 ± 4	yes <sup>f</sup>	11
May 13, 1972	45.13	28.11	3	11 ± 5	5 ± 2	yes <sup>f</sup>	
April 21, 1975	45.42	27.95	3	16 ± 6	3 ± 3	no	
Sept. 1, 1979	44.96	28.06	6	11 ± 6	9 ± 3	no	
April 7, 1975	42.59 ± 0.016	29.44 ± 0.009	8	29 ± 6	16 ± 3	no	12
Sept. 10, 1979	42.74	29.29	7	10 ± 7	15 ± 3	no	
Jan. 20, 1968	41.30 ± 0.020	29.33 ± 0.013	7	16 ± 8	15 ± 7	no	13
June 10, 1975	40.73	29.41	3	2 ± 3	9 ± 4	yes	
March 9, 1984	40.70	29.42	3	2 ± 3	16 ± 4	no	
Jan 18, 1985	29.94 ± 0.022	42.73 ± 0.019	6	10 ± 3	17 ± 8	no	14
March 11, 1966	28.33 ± 0.012	43.87 ± 0.009	6	10 ± 4	5 ± 5	yes	
Feb. 17, 1967	28.87	43.44	3	10 ± 5	3 ± 3	yes	15
Jan. 15, 1984	28.86	43.45	3	10 ± 3	6 ± 3	yes <sup>f</sup>	
March 15, 1984	28.45	43.75	3	9 ± 5	6 ± 5	yes	
May 15, 1974	27.38 ± 0.014	44.28 ± 0.010	25	20 ± 4	26 ± 6	no	16
July 13, 1985	25.92 ± 0.020	45.04 ± 0.021	5	8 ± 5	3 ± 5	yes <sup>f</sup>	
June 28, 1977	22.65 ± 0.015	45.08 ± 0.010	5	10 ± 3	10 ± 3	no	18
Jan. 19, 1982	21.56 ± 0.026	45.42 ± 0.015	5	13 ± 6	20 ± 6	no	

Joint relocation was performed for swarms grouped as shown. Groups are listed in order of decreasing latitude, one group per figure. Swarms are listed chronologically within groups and are identified by the date of the first relocated event in the series.

<sup>a</sup> Epicentroid is calculated for each swarm individually. Standard deviations given for first swarm in each group apply to all swarms in that group.

<sup>b</sup> Number of events relocated.

<sup>c</sup> Length (km) of the area of activity during the swarm, measured parallel to the strike of the median valley, taken as the greatest separation (projected on the desired direction) between any two events in the swarm. In several swarms, poorly-located outliers have been ignored for this purpose. Uncertainty is one standard deviation. See discussion in text.

<sup>d</sup> Width (km) of the area of activity during the swarm, measured perpendicular to the strike of the median valley. See note c.

<sup>e</sup> Test of null hypothesis that all events in a swarm have zero-length cluster vectors, i.e., all the events occurred at a common point. A swarm is considered point-like if the null hypothesis cannot be rejected at the 99% confidence level.

<sup>f</sup> These swarms are point-like at the 99% confidence level, but not at the 95% confidence level. See *Jordan and Sverdrup* [1981] for further information on this test.

The 34 swarms selected for analysis are listed in Table 1. The approximate locations of the swarms on the MAR are shown in Figures 1–5. Most of the events have magnitudes in the range  $4.3 \leq m_b \leq 5.0$ , but earthquakes as small as  $m_b = 3.9$  and as large as  $m_b = 5.9$  are included. In the late 1960s the detection threshold (above which detection is nearly complete) of the global seismic network was about  $m_b = 4.7$  for earthquakes on the northern MAR [Evernden, 1969]. The detection threshold has gradually decreased (with significant fluctuations) since the early 1960s [Habermann, 1982], but it is currently probably no lower than  $m_b = 4.5$  on average over the region of this study.

#### Multiple Event Location

The relative locations of the earthquakes in the selected swarms are determined by simultaneous relocation using the

technique of hypocentroidal decomposition [Jordan and Sverdrup, 1981]. The location problem is separated into two parts: (1) estimation of the relative locations (cluster vectors) within the cluster from differences between the observed travel times from two or more members of the cluster to each station, and (2) estimation of the absolute location of the hypocentroid (the centroid of the cluster vectors) using the full set of observed arrival times. Compared with other techniques for relative event location, hypocentroidal decomposition is especially powerful for the study of smaller, sparsely recorded events because it makes optimal use of all the available arrival time data.

The absolute locations (i.e., the hypocentroid of the cluster) determined by hypocentroidal decomposition are subject to the same sources of bias as any teleseismic location: errors in the theoretical travel times coupled with

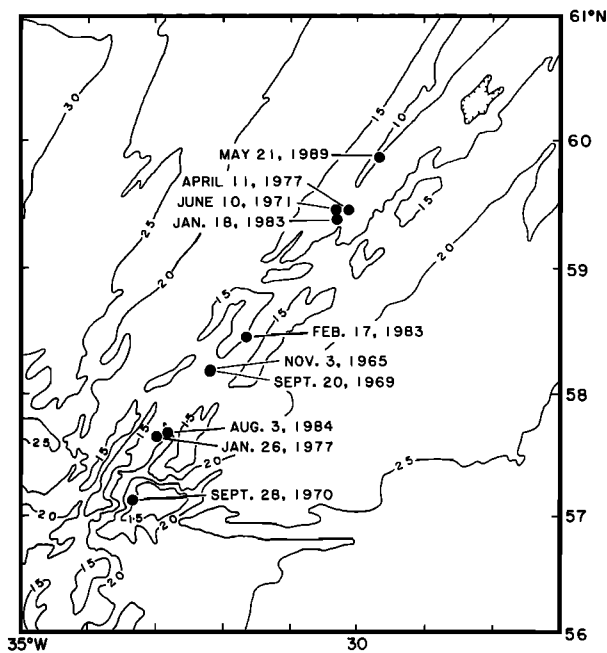


Fig. 1. Epicentroids of 10 teleseismically located swarms on the Reykjanes Ridge. Bathymetry, shown by selected 1-, 1.5-, 2-, and 2.5-km isobaths, is from *Laughton and Monahan* [1978].

unbalanced station distribution can easily lead to a bias of 10 km or more [*Herrin and Taggart*, 1968; *Phillips et al.*, 1979]. We determine theoretical travel times from the *Herrin* [1968] tables, corrected for ellipticity [*Dziewonski and Gilbert*, 1976] and incorporating the azimuthally-dependent station corrections (for applicable stations) of *Dziewonski and Anderson* [1983]. Relocations of earthquakes on the Kane transform fault [*Bergman et al.*, 1988] and comparison of the teleseismic relocation for one swarm in this study with locations calculated from a local ocean bottom seismograph network [*Kong et al.*, 1988] suggest that the epicentroids may be systematically biased to the north by as much as 15 km, because of the concentration of seismic stations in the northern hemisphere. Longitudinal bias appears to be small, as expected from the approximately equal distributions of seismic stations in North America and Europe.

Hypocentroidal decomposition is as vulnerable to the strong tradeoff between focal depth and origin time as single-event location with teleseismic data. Considering the consistent results of microearthquake studies [e.g., *Toomey et al.*, 1985] and body waveform modelling studies of larger events [*Huang and Solomon*, 1988], it is reasonable to assume that most mid-ocean ridge earthquakes have focal depths within the upper 10 km of the oceanic crust and upper mantle. We therefore fixed the depth of all events in this study at 10 km below sea level, corresponding to a depth of 6–7 km beneath the seafloor of the median valley. Errors in the assumed depth are unlikely to exceed 5 km and will be absorbed in the origin time; the epicentral components of the relative locations are insensitive to depth errors of this magnitude.

Most of the relocations are performed with P wave arrival time data from seismic stations in the range  $20^\circ < \Delta < 98^\circ$ . European seismic stations have epicentral distances as short as  $\Delta \sim 20^\circ$  from swarms in the northern part of the study

region (north of about  $40^\circ\text{N}$ ). For swarms at latitudes less than about  $30^\circ\text{N}$  on the MAR, there are virtually no stations closer than  $\Delta \sim 30^\circ$ . The relocation of the May–June 1989 swarm and the three other swarms relocated with it employed data from stations as near as  $\Delta \sim 5^\circ$  (see above), and data from several stations as near as  $\Delta \sim 12^\circ$  were used in the relocation of the March 9, 1967, swarm. Inclusion of data at  $\Delta < 30^\circ$  (the traditional lower bound for “teleseismic” studies) is critical to achieve the azimuthal coverage necessary for satisfactory location of many of the smaller events in the study, particularly those on the Reykjanes Ridge. Arrival time data are weighted inversely to the precision of the reported arrival time. Data reported to the nearest second are assigned a standard error of 1.0 s, while data given to the nearest 0.1 s are assigned a standard error of 0.5 s. With the exception of the May–June 1989 swarm, for which PDE hypocenters are used, ISC epicenters and origin times are adopted as the initial values in the relocations. In the estimation of the epicentroid (depth is fixed), data with a residual less than 10 s are used at the first iteration; a 3 s cutoff is used for subsequent iterations. After convergence, the path-corrected residuals used to estimate corrections to the cluster vectors are inspected to identify outliers, which are flagged. The entire process is repeated several times (with flagged data dropped from the cluster vector calculation) until the distribution of path-corrected residuals is approximately normal.

The ability to resolve the relative locations of the earthquakes in a cluster depends on the number, “connectedness,” and azimuthal distribution of arrival time data. In general, the reliability of relocations for events with less than about 20 arrival times is questionable. In some cases, the quality and distribution of a smaller number of data produce a solution with nominally acceptable parameter variances; the true uncertainty is undoubtedly greater, however. The minimum requirement for connectedness is that a station reporting an arrival time for a particular event also have reported an arrival time for at least one other event in the

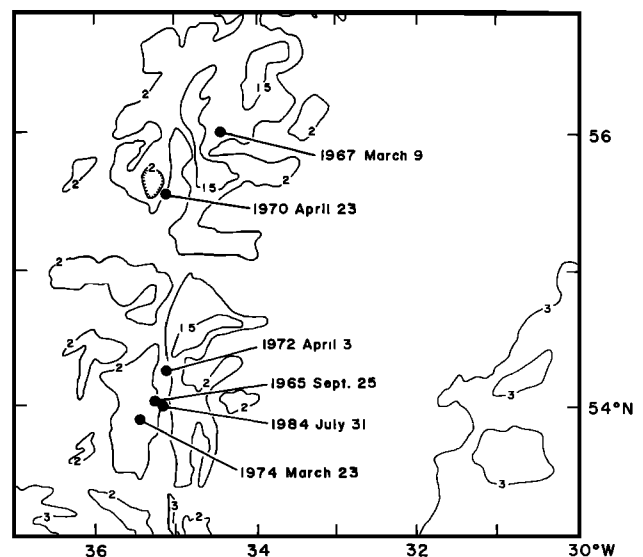


Fig. 2. Epicentroids of six teleseismically located swarms on the Reykjanes Ridge. Bathymetry, shown by selected 1.5-, 2-, and 3-km isobaths, is from *Laughton and Monahan* [1978].

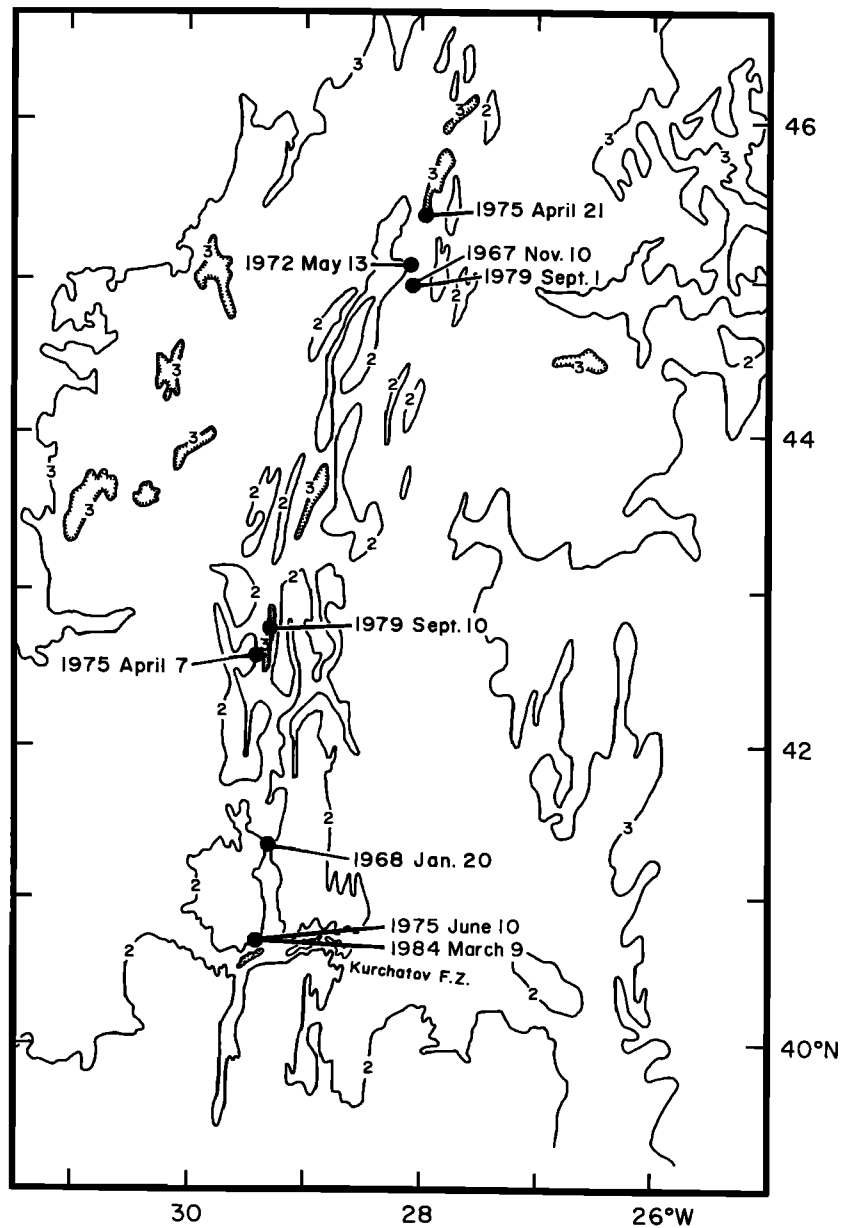


Fig. 3. Epicentroids of nine teleseismically located swarms on the Mid-Atlantic Ridge north of the Azores triple junction. Bathymetry, shown by selected 2- and 3-km isobaths, is from *Searle et al.* [1982].

cluster. Higher connectedness improves the estimate of a station's path bias, which is removed from all data prior to estimating corrections to the cluster vectors. A reliable (relative) location is usually not possible with a gap of more than  $180^\circ$  in the azimuthal distribution of data; in such a case the family of confidence ellipses for the spatial components of the cluster vector will be extremely elongated along an axis bisecting the gap in data. Because of these factors, some of the swarm earthquakes found in our search of the ISC catalog could not be relocated with an accuracy sufficient for tectonic interpretation, and such events are not included in the analysis.

Details of the individual relocations are discussed in the appendix, which also includes the epicenters for all the relocated swarm earthquakes (222 events). The cluster vectors and their 95% confidence ellipses are shown in Figures 6–19.

#### CHARACTERISTICS OF RIDGE EARTHQUAKE SWARMS

The primary test of the hypothesis that teleseismically detected swarms on mid-ocean ridges are marine examples of dike-intrusion swarms in volcanic rift zones exploits the characteristic geometry of well-studied volcanic swarms and the tendency for the seismicity to track the movement of the magma front down the rift zone. Secondary evidence arises from comparisons of the durations of swarms and the timing of seismic activity during swarms, the characteristic magnitudes of earthquakes, their fault mechanisms, and their locations relative to the axis of accretion.

#### *Geometry of Swarms*

Terrestrial dike swarms and their associated earthquake swarms are elongated, with typical widths of a few kilometers and lengths of up to several tens of kilometers. For

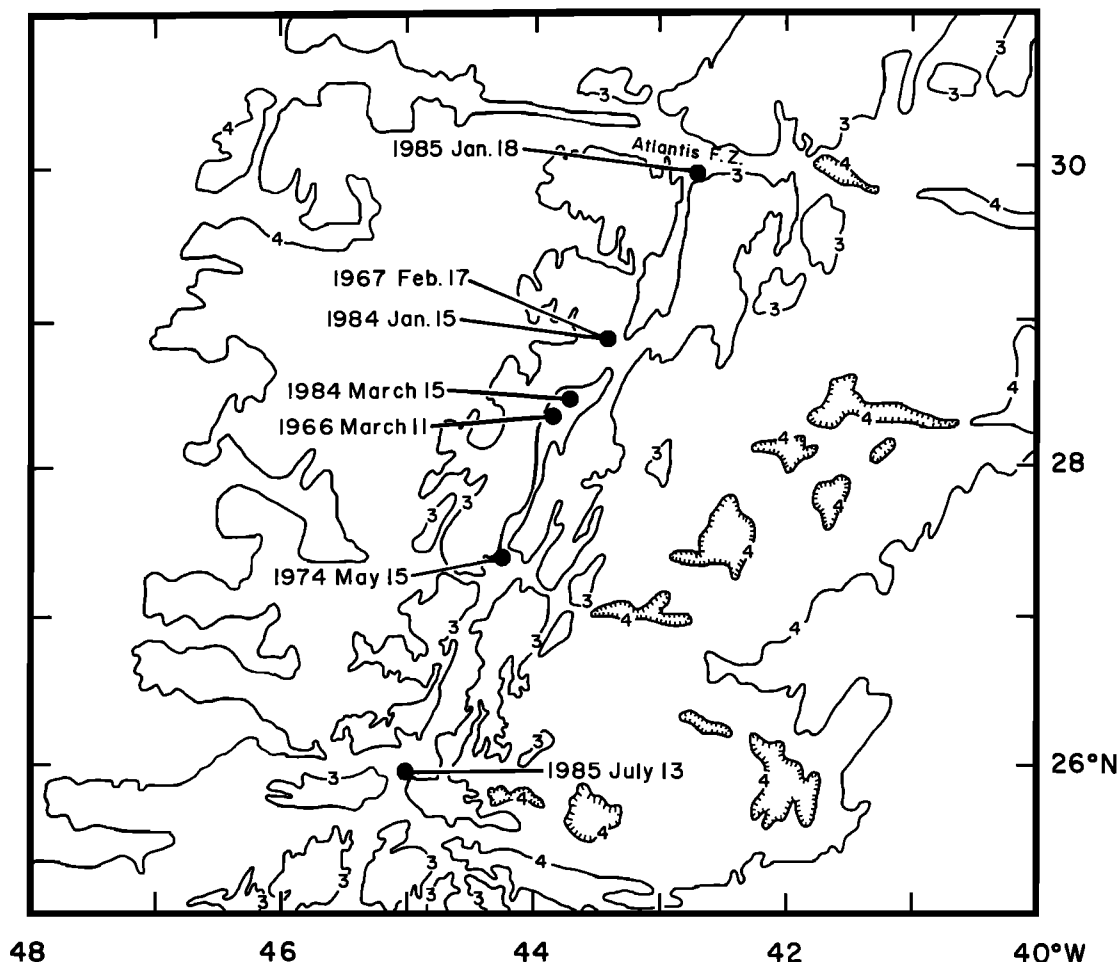


Fig. 4. Epicentroids of seven teleseismically located swarms on the Mid-Atlantic Ridge south of the Atlantis Fracture Zone. Bathymetry, shown by selected 3- and 4-km isobaths, is from *Searle et al.* [1982].

comparison, we seek a measure of the degree of elongation in the clusters of mid-ocean ridge earthquake swarms. To the extent that these earthquakes are associated with dike emplacement, any such elongation can be expected to occur along the axis of the median valley, an orientation which can be determined with reasonable accuracy from the bathymetry. A simple measure of the degree of elongation is the aspect ratio of the cluster of epicenters, the ratio of the length (along the strike of the ridge axis) to the width (across strike). To measure these dimensions, the spatial components of the cluster vectors and their covariance matrix are rotated into a coordinate frame with one axis parallel to the ridge axis. The separation of the two outlying events in each coordinate and the variance of that separation are calculated. This estimate of variance is at best a weak substitute for the true uncertainty of the spatial extent of the swarm in an arbitrary direction, since it uses only a small fraction of the information contained in the entire set of cluster vectors. When an outlier has been located with a small number of data and lies well outside the remainder of the cluster, another member of the swarm was chosen as a more robust indicator of swarm dimensions. These cases are noted in the appendix. The dimensions reported (Table 1) are thus intended to be robust estimates of minimum swarm dimensions. Because of the distribution of seismic stations with respect to the study area, the minor axis of the cluster vector

confidence ellipse is oriented approximately perpendicular to the trend of the ridge axis for most events. Therefore, estimates of the cross-axis extent of the swarms generally have smaller uncertainties than estimates of the along-axis extent.

Some bias in our estimated swarm dimensions may arise from discrepancies between the true velocity structure in the source region and the velocity structure implicit in the *Herrin* [1968] tables used to calculate travel times and ray parameters. On average, the shallow velocity structure of the mid-ocean ridge is faster than the *Herrin* velocity structure, which assumes crustal velocities to a depth of 40 km [*Herrin et al.*, 1968]; in this case the separation between events will be underestimated by the relocation procedure. Any such bias is proportional to the separation between events; it should be negligible for the estimates of cross-axis swarm dimensions, which are generally small, but may be significant for the along-axis dimension for some of the larger swarms. Where several swarms have been jointly relocated, the separation between the swarms may tend to be underestimated for this reason.

The estimated widths (cross-axis) and lengths (along-axis) for the 34 MAR swarms are plotted in Figure 20. There is a weak positive correlation between width and length (correlation coefficient = 0.43), and little tendency for swarms to be elongated along the strike of the median valley. Only

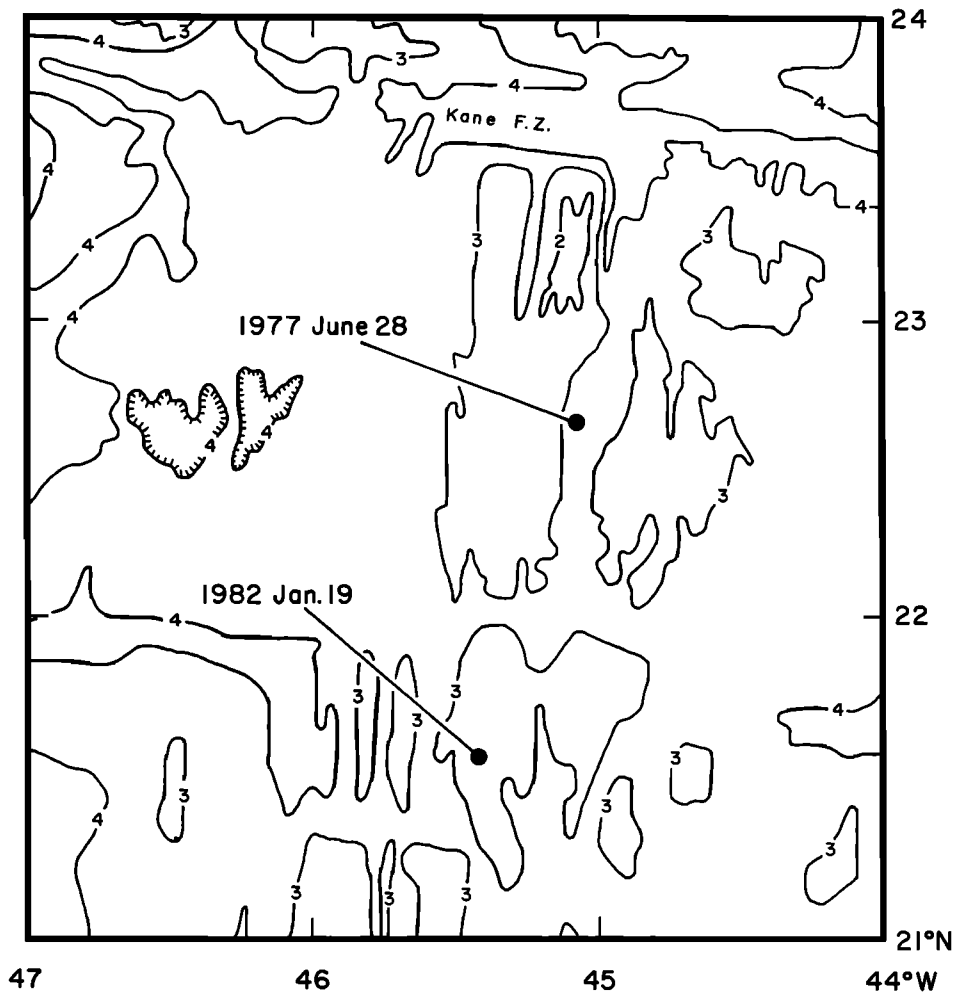


Fig. 5. Epicentroids of two teleseismically located swarms on the Mid-Atlantic Ridge south of the Kane fracture zone. Bathymetry, shown by selected 2-, 3-, and 4-km isobaths, is from Searle *et al.* [1982].

seven swarms lie significantly outside the region defined by having both width and length less than 15 km, and only one of these (March 9, 1967) has dimensions (45 km by 10 km) similar to those of larger volcanic rift zone swarms; the width of this last swarm is probably underestimated (see appendix). None of the swarms have both width and length less than 5 km, but this does not rule out the possibility that some of the swarms may represent seismicity confined effectively to a point. Jordan and Sverdrup [1981] describe a statistical test of the null hypothesis that all members of a swarm have cluster vectors of zero length. The results of this calculation for the swarms of this study are listed in Table 1. In general, swarms for which both the width and length are less than 10 km cannot be distinguished from points of activity at a high level of confidence; the estimated widths and lengths of such swarms may have little meaning. For 19 swarms, indicated by open circles in Figure 20, the null hypothesis can be rejected at a confidence level exceeding 99%.

Terrestrial volcanic rift zones typically have widths of 5 km or less, comparable to that of the inner rift valley of the MAR. Although there is evidence that volcanism occasionally occurs as much as 20 km from the long-term locus of the axis [Macdonald, 1977; Atwater, 1979], we can take as a

fairly strong constraint that an earthquake swarm directly associated with intrusive volcanism on the MAR should have a width less than about 5 km. Of the 34 swarms, this criterion is met by the 15 for which the point-source hypothesis cannot be rejected (see above), as well as by three swarms which are non-pointlike (Figure 20). Of these 18 cases, however, 15 contain only three relocated earthquakes; the apparent narrowness of some of these swarms is undoubtedly a product of small sample size. On the basis of width, therefore, at least half of the swarms can be discounted as purely volcanic swarms.

#### Migration of Swarm Seismicity

For those swarms which may have widths less than 5 km, migration along axis (presumably away from a central magma chamber) would be strong evidence for association with an episode of dike emplacement. Of the 18 candidate swarms, only three can be clearly distinguished from point sources (April 21, 1975; April 11, 1977; July 31, 1984); any apparent space-time migration pattern in the remaining swarms is probably spurious. There is a clear linear progression from north to south in the July 31, 1984, swarm (Figure 8). Given the uncertainties in the relative locations, a pro-

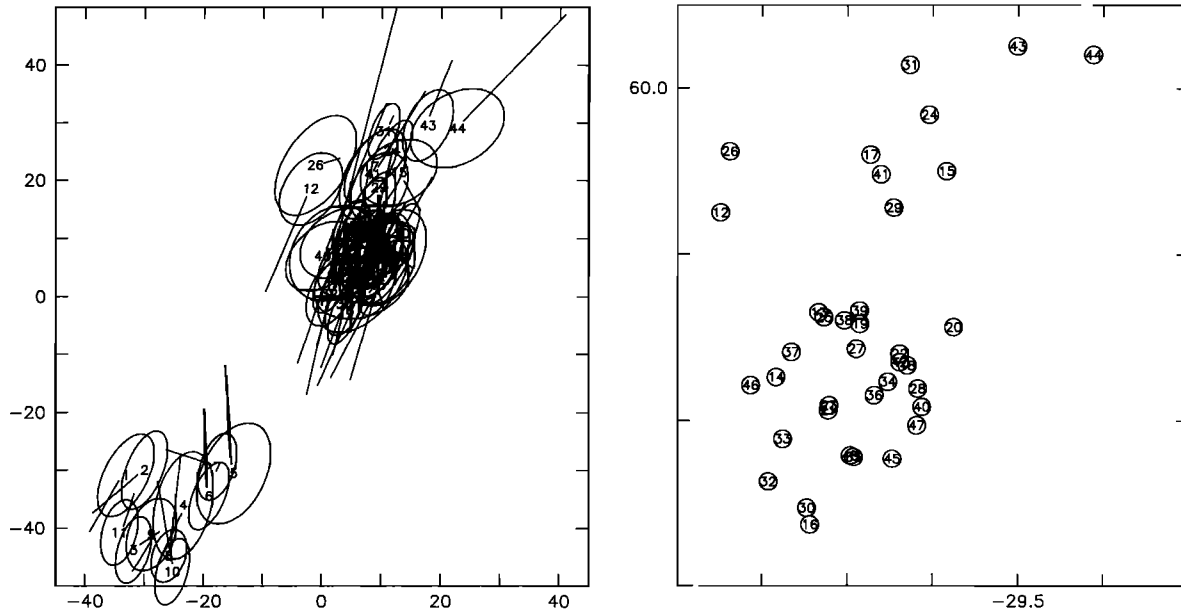


Fig. 6. (a) Relative locations of earthquakes in the swarms of June 10, 1971 (#1-4), April 11, 1977 (#5-8), January 18, 1983 (#9-11), and May 21, 1989 (#12-48). For each earthquake the relative location of the epicenter is indicated by the event number, the 95% confidence ellipse for the cluster vector is shown, and the change in relative position from the starting (ISC) location is indicated by a line. The initial epicenters for the May 21, 1989, swarm are from the NEIS Preliminary Determination of Epicenters. The epicentroid for all relocated events in the four swarms is at (0,0) km (cross). (b) Absolute locations of the earthquakes in the May 21, 1989, swarm. Tic marks are at intervals of  $0.1^\circ$  in latitude and longitude.

gression cannot be ruled out for the April 21, 1975, swarm (Figure 9). Since both swarms contain only three relocated events, however, the significance of these patterns must be discounted. The four events in the April 11, 1977, swarm are consistent with a north-south migration (Figure 6). None of the swarms with widths greater than 5 km show any clear pattern of space-time progression along the ridge axis.

#### Duration

To determine the duration of each swarm, we compiled a complete list (from the ISC catalog) of all constituent events, with no minimum on the number of teleseismic arrival time data (the March 9, 1967, swarm was an exception; see the appendix). While the number of detected events in a swarm strongly reflects spatial and temporal variations in the detec-

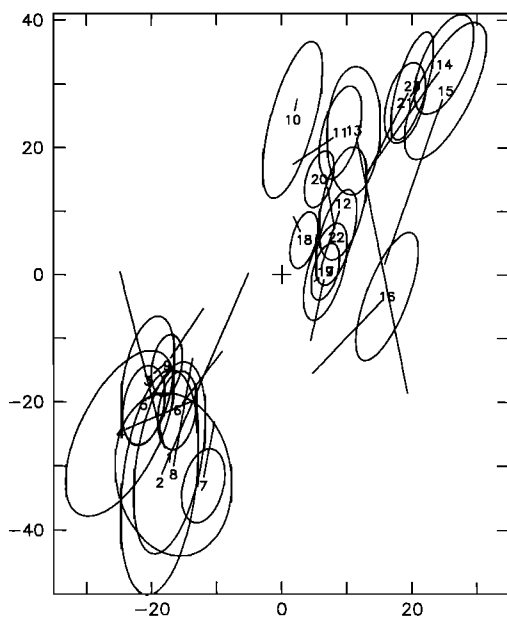


Fig. 7. Relative locations of earthquakes in the swarms of November 3, 1965 (#1-3), September 20, 1969 (#4-9), and February 17, 1983 (#10-23). See Figure 6 for further explanation.

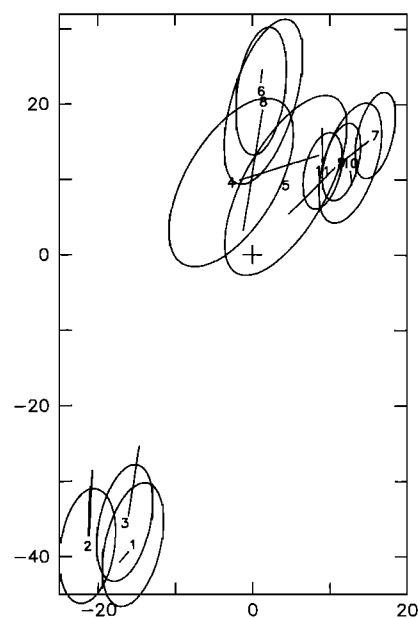


Fig. 8. Relative locations of earthquakes in the swarms of September 28, 1970 (#1-3), January 26, 1977 (#4-6), and August 3, 1984 (#7-11). See Figure 6 for further explanation.

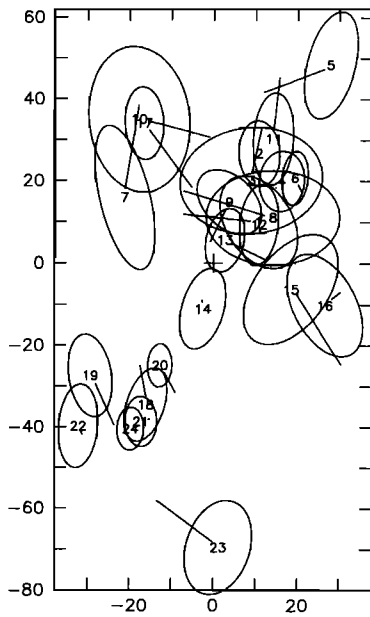


Fig. 9. Relative locations of earthquakes in the swarms of March 9, 1967 (#1-17), and April 23, 1970 (#18-24). See Figure 6 for further explanation.

tion threshold of the global seismic network, the duration is less sensitive to these factors. The duration of each swarm and the number of constituent events are shown in Figure 21. Most of the swarms contain fewer than eight earthquakes and last less than 2-3 days. Several sites have experienced swarms at intervals of a few years (Table 1); such a pattern is also observed during some terrestrial eruptive episodes (e.g., the 1975-1984 Krafla swarms). For most of the swarms, the largest fraction of the seismicity occurs within one day of the first event. This observation also holds true

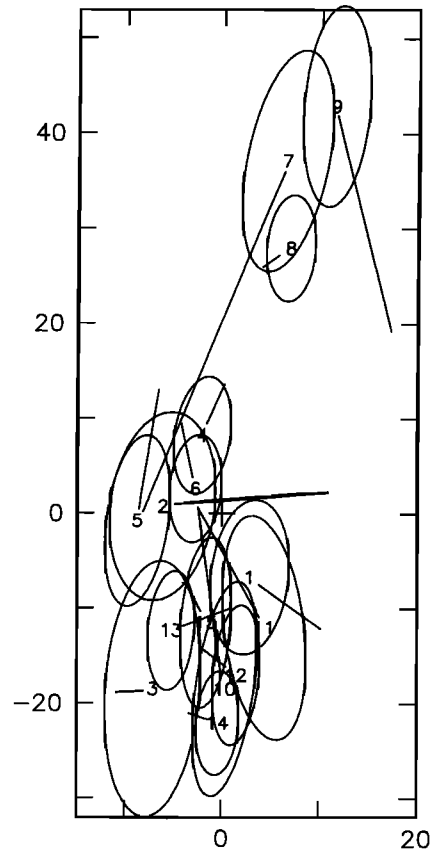


Fig. 11. Relative locations of earthquakes in the swarms of November 10, 1967 (#1-3), May 13, 1972 (#4-6), April 21, 1975 (#7-9), and September 1, 1979 (#10-15). See Figure 6 for further explanation.

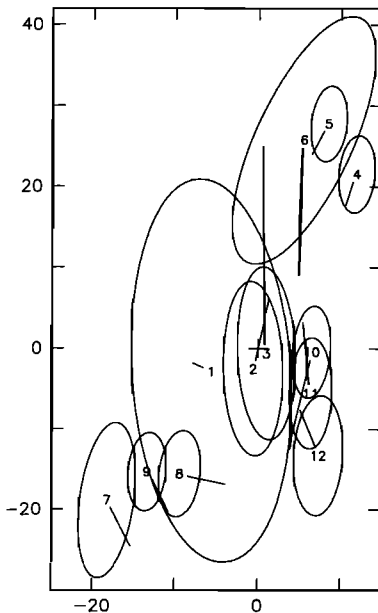


Fig. 10. Relative locations of earthquakes in the swarms of September 25, 1965 (#1-3), April 3, 1972 (#4-6), March 23, 1974 (#7-9), and July 31, 1984 (#10-12). See Figure 6 for further explanation.

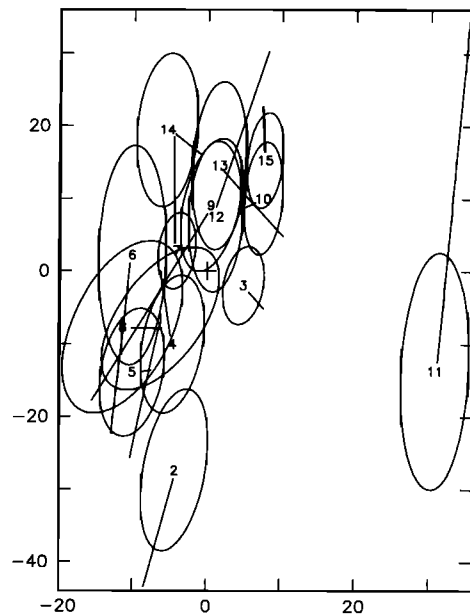


Fig. 12. Relative locations of earthquakes in the swarms of April 7, 1975 (#1-8), and September 10, 1979 (#9-15). See Figure 6 for further explanation.

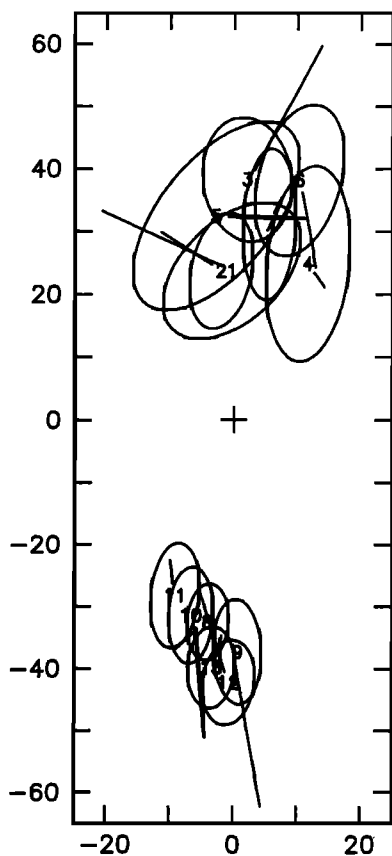


Fig. 13. Relative locations of earthquakes in the swarms of January 20, 1968 (#1-7), June 10, 1975 (#8-10), and March 9, 1984 (#11-13). See Figure 6 for further explanation.

for the longest swarms (Figure 22), whose greater duration in most cases results from a small number of later events. The patterns of seismic activity versus swarm duration of the longer and larger mid-ocean ridge swarms shown in Figures 21 and 22 are similar to those observed in teleseismically observed swarms in Iceland (57 events in 40 days and 19 events in 15 days for the December 24, 1975 and January 9, 1978, swarms, respectively) and the Afar (10 events in 40 days during the November 7, 1978, swarm). The duration (20 days) of the June 12, 1968, Fernandina swarm in the Galapagos Islands is also similar to that of the longer mid-ocean ridge swarms, but the number of earthquakes (~280) is far higher; the relevance to mid-ocean ridge seismicity of the caldera collapse model put forward to explain this swarm by Francis [1974] is uncertain.

### Magnitudes

The largest members of the mid-ocean ridge swarms are consistently greater in magnitude than the largest events observed in purely volcanic swarms in Iceland or Hawaii. In particular, the 18 swarms with widths (possibly) less than 5 km have maximum magnitudes ranging from  $m_b = 4.7$  to 5.3, whereas earthquakes associated with dike swarms in Iceland and Hawaii seldom exceed  $m_b = 4.0$ . In both Iceland and Afar, however, rifting events have been accompanied by swarms of earthquakes whose number and magnitudes are comparable to those of mid-ocean ridge swarms (see above).

### Faulting Style

Focal mechanisms are known for many of the larger swarm events in this study (see the appendix); normal faulting is typical, especially for the best-recorded events. Of the 18 swarms in this study which, on the basis of width, are most likely to be volcanic in origin, four are known to have at least one earthquake with a normal faulting mechanism. Several of the swarms studied here (e.g., September 20, 1969; June 28, 1977) contain large ( $m_b > 5.4$ ) normal faulting earthquakes which from a seismological point of view are indistinguishable from the isolated large normal-faulting earthquakes generally interpreted as indicative of extension across the mid-ocean ridge median valley [Solomon *et al.*, 1988]. The largest earthquakes in the 1978 swarm in the Ghoubbet-Asal Rift were characterized by normal faulting. The observed ground deformation suggests that there was a significant component of normal faulting involved in the two large earthquake swarms in the rift zone north of Krafla caldera in Iceland [Sigurdsson, 1980]. In contrast, evidence from Hawaii and Iceland suggests that many of the earthquakes directly related to magma injection into dike swarms are characterized by strike-slip faulting [Klein *et al.*, 1977; Karpin and Thurber, 1987]. Strike-slip faulting has also been reported for earthquakes in a teleseismically located swarm in the northern Gulf of California [Tatham and Savino, 1974], but the swarm may have occurred on a transform segment of the plate boundary.

The style of faulting may be one of the more useful clues to classification of an earthquake swarm as "tectonic" or "volcanic." Normal faulting is, of course, the dominant mode of brittle deformation of a lithospheric plate under extension. The sense of faulting predicted by the magma injection model of Hill [1977] depends on the orientation of dikes with respect to the free surface and the regional stress system. For a system of shallow, vertical, en echelon dikes extending along a narrow rift zone, Hill's model can account for the observations of strike-slip faulting in volcanic swarms in a rather natural way, but the dike geometry necessary to produce normal faulting at the scale required for teleseismically observed earthquakes is incompatible with the shallow depth extent of dikes and earthquakes on the mid-ocean ridge. The possibility that some of the smaller events in the

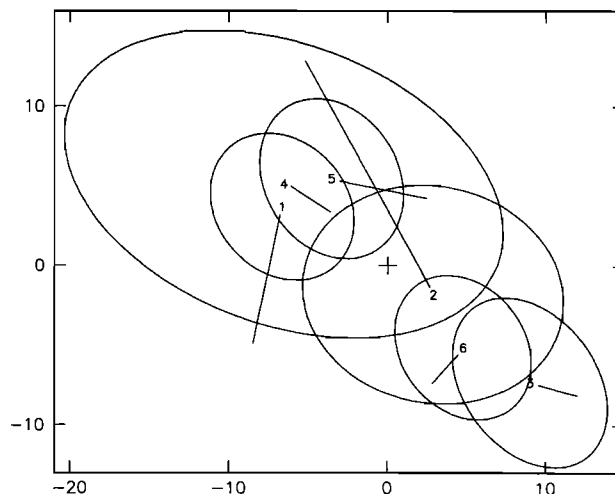


Fig. 14. Relative locations of earthquakes in the swarm of January 18, 1985. See Figure 6 for further explanation.

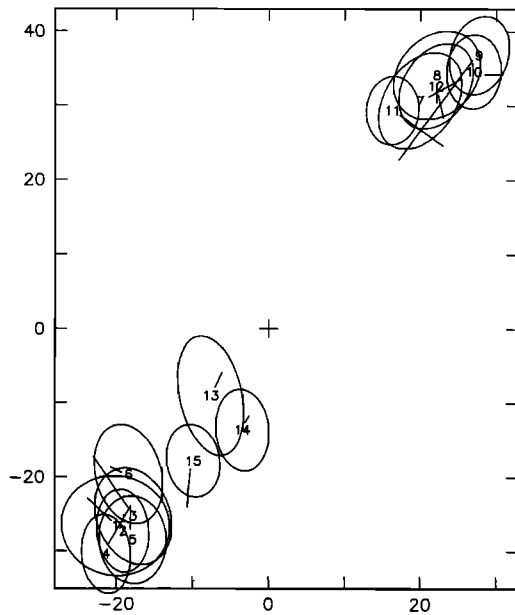


Fig. 15. Relative locations of earthquakes in the swarms of March 11, 1966 (#1–6), February 17, 1967 (#7–9), January 15, 1984 (#10–12), and March 15, 1984 (#13–15). See Figure 6 for further explanation.

present study could have strike-slip mechanisms cannot be rejected. Given the dominantly extensional tectonics of mid-ocean ridges, observation of median valley earthquakes with strike-slip mechanisms would constitute strong evidence for association with an activated dike system.

#### Location Relative to the Axis of Accretion

Dike intrusion (and associated seismicity) on the mid-ocean ridge system should be localized close to the neovolcanic zone, within the inner floor of the median valley. The epicenters of the mid-ocean ridge swarms are generally consistent with locations overlapping the inner floor, but uncertainty in the epicentroid is large enough to encompass alternative models, such as locations between the inner and outer rift walls, in many cases. In several areas, however, two colocated swarms are clearly separated in the cross-axis direction by 5 km or more (e.g., June 10, 1971 and April 11, 1977, swarms, Figure 6a; January 26, 1977, and August 3, 1984, swarms, Figure 8; May 13, 1972, and September 1, 1979, swarms, Figure 9; September 25, 1965, and July 31, 1984, swarms, Figure 10). Such a pattern, which is observed for at least five of the relatively narrow, potentially volcanic, swarms, is not consistent with a volcanic origin for both swarms unless one admits the hypothesis that the axis of magmatism can migrate across the inner floor over periods of a few years. An alternative explanation is that one swarm represents volcanic activity in the inner floor while the second is an expression of extensional tectonism elsewhere in the median valley. It is more likely, however, that these observations reflect a single pattern of deformation which has substantial cross-axis dimensions, namely extensional tectonism. One swarm can be localized outside the inner floor with some confidence: the March 23, 1974, swarm is colocated with three other swarms (Figure 10) on a distinctly linear ridge segment (Figure 2). We interpret the pattern of

relative locations, in combination with the bathymetry, to indicate that the three other swarms probably are located within or close to the inner floor, while the 1974 swarm occurred to the west, in the terraces between the inner and outer rift walls or within the rift mountains. This observation supports the view that extensional tectonism on the MAR can give rise to swarm-type seismicity.

In contrast to the other swarms in this study the May 21, 1989, swarm (and, to a lesser extent, the other three swarms relocated with it), is located on a section of the Reykjanes Ridge where the ridge axis has an elevated, triangular profile rather than the rifted median valley characteristic of most of the MAR (Figure 1). This morphology, shared by other oceanic ridge segments near hotspots, has been interpreted as an expression of "pipe" flow along the axis southward from Iceland [Vogt, 1971; Vogt and Johnson, 1975]. Earthquake swarms are observed on this section of the ridge but the seismicity rate is much lower than that of the more typical MAR south of about 60°N [Francis, 1973]. Despite the contrast in ridge morphology, we find little seismic evidence to suggest that the origin of this swarm differs from that of other swarms to the south; a strike-slip focal mechanism has been reported for the largest event in this swarm [Dziewonski *et al.*, 1989], but a normal faulting mechanism is equally consistent with the data (see appendix).

#### DISCUSSION

Consideration of the various characteristics of mid-ocean ridge swarms leads us to the conclusion that these earthquakes bear little resemblance to earthquakes resulting directly from the lateral motion of magma through crustal-level dike systems during volcanic episodes at well-studied terrestrial rift zones in Iceland or Hawaii. Such earthquakes are seldom recorded at teleseismic distances from these rifts, and we conclude that the same is true of purely volcanic swarms on the MAR. In contrast, the teleseismically-observable characteristics of mid-ocean ridge swarms are

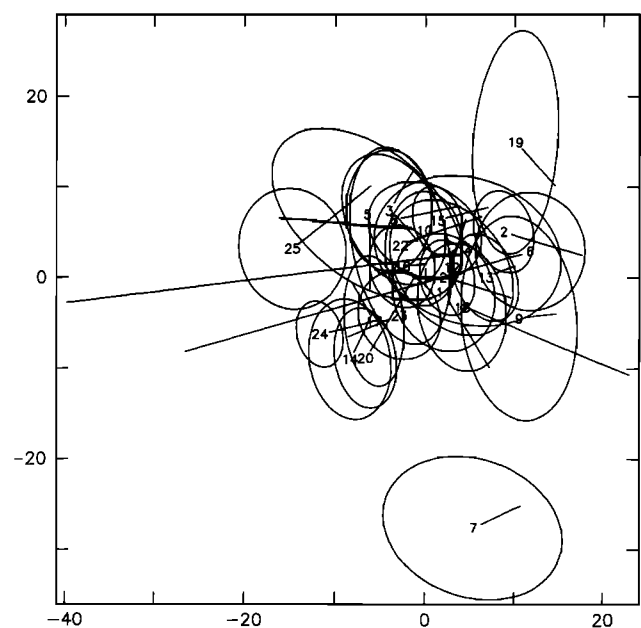


Fig. 16. Relative locations of earthquakes in the swarm of May 15, 1974. See Figure 6 for further explanation.

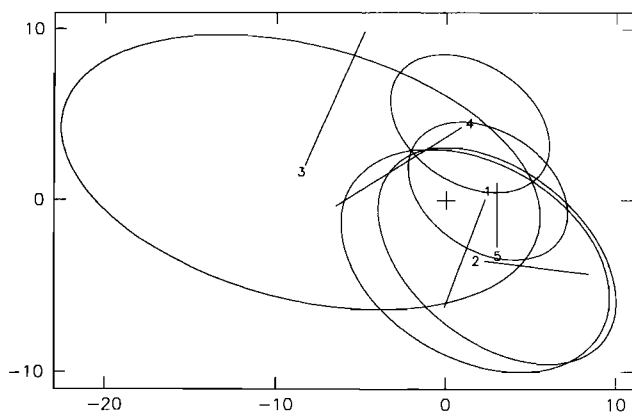


Fig. 17. Relative locations of earthquakes in the swarm of July 13, 1985. See Figure 6 for further explanation.

easily accommodated within a model which treats them as expressions of extensional tectonism, in particular the development of the topographic relief of the median valley and rift mountains. There is clear evidence from Iceland that major eruptive episodes may be accompanied by earthquake swarms indistinguishable from the mid-ocean ridge swarms of this study, but the 1978 Afar swarm was accompanied only by minor volcanism of a passive nature [Ruegg *et al.*, 1979]. The only site of a mid-ocean ridge swarm (June 28, 1977) to be carefully surveyed by high-resolution bathymetric mapping and microearthquake characterization shows no signs of recent magmatism or volcanism [Toomey *et al.*, 1988]. We propose that the dominant factor linking the larger swarms of Iceland and the Afar and those of the mid-ocean ridge is the regional extensional stress field and the development of a rifted morphology at the axis of accretion. The frequency with which such rifting is accompanied by significant volcanism is unknown.

Most of the topography of the MAR is created at the inner and outer rift walls, on scarps composed of numerous closely-spaced normal faults with throws of up to several hundred meters [Macdonald, 1986]. Some considerable fraction of mid-ocean ridge seismicity must be involved in creating these scarps. It is natural to suppose that this

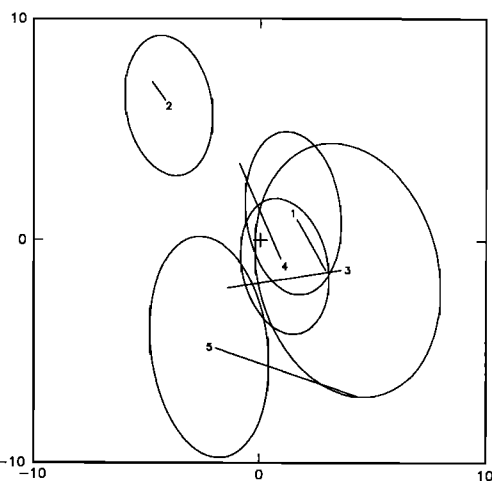


Fig. 18. Relative locations of earthquakes in the swarm of June 28, 1977. See Figure 6 for further explanation.

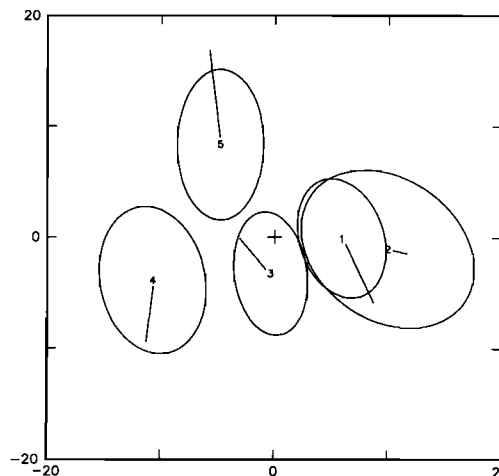


Fig. 19. Relative locations of earthquakes in the swarm of January 19, 1982. See Figure 6 for further explanation.

fraction includes the largest earthquakes ( $5.4 \leq m_b \leq 6.0$ ), which have been thoroughly studied by Huang *et al.* [1986], Jemsek *et al.* [1986], and Huang and Solomon [1987, 1988]. The swarms studied here include some of these larger earthquakes, which invariably have normal faulting focal mechanisms, and we can find no seismological evidence to suggest that the tectonic role of other swarm events differs significantly from that of the largest ridge earthquakes. From observations of water reverberations which allow an independent estimate of water depth above the source, it appears that the largest ridge-axis earthquakes usually occur near, if not within, the inner floor of the median valley. The depth range of coseismic faulting inferred from centroid depths is 2–10 km, which requires that a considerable amount of cooling of the newly emplaced crustal material must take place before such large events can occur. At slow spreading rates, hydrothermal circulation appears capable of cooling a volume of crust large enough to fail in an earthquake with  $m_b \sim 5.5$  within perhaps 5–10 km of the accretion axis [Phipps Morgan *et al.*, 1987; Lin and Parmentier, 1989]. Access for seawater to a significant volume of the crust is likely provided by the intense fissuring which occurs in the newly-emplaced crustal material between the neovolcanic zone and the inner rift walls [Luyendyk and Macdonald, 1977; Ballard and van Andel, 1977].

We support the view that the largest normal-faulting ridge-axis earthquakes occur on the faults marking the inner rift wall and that they are the dominant events in the development of these faults (see also Huang and Solomon [1988]; Toomey *et al.* [1988]). This hypothesis is consistent with the spatial patterns of teleseismically located swarms, evidence from detailed source studies of the largest ridge earthquakes, and knowledge of the structure of the median valley. The preferential occurrence of the largest events on these faults can be explained by noting that prior to this faulting the newly formed crust is relatively homogeneous, having never before been significantly faulted. Because these earthquakes may nucleate at depths of 5–6 km below the sea floor on faults dipping inward at  $\sim 45^\circ$ , their epicenters may lie near the center of the inner floor of the median valley. Beyond the inner rift wall the crust is thoroughly disrupted into narrow fault slivers which may be too weak to

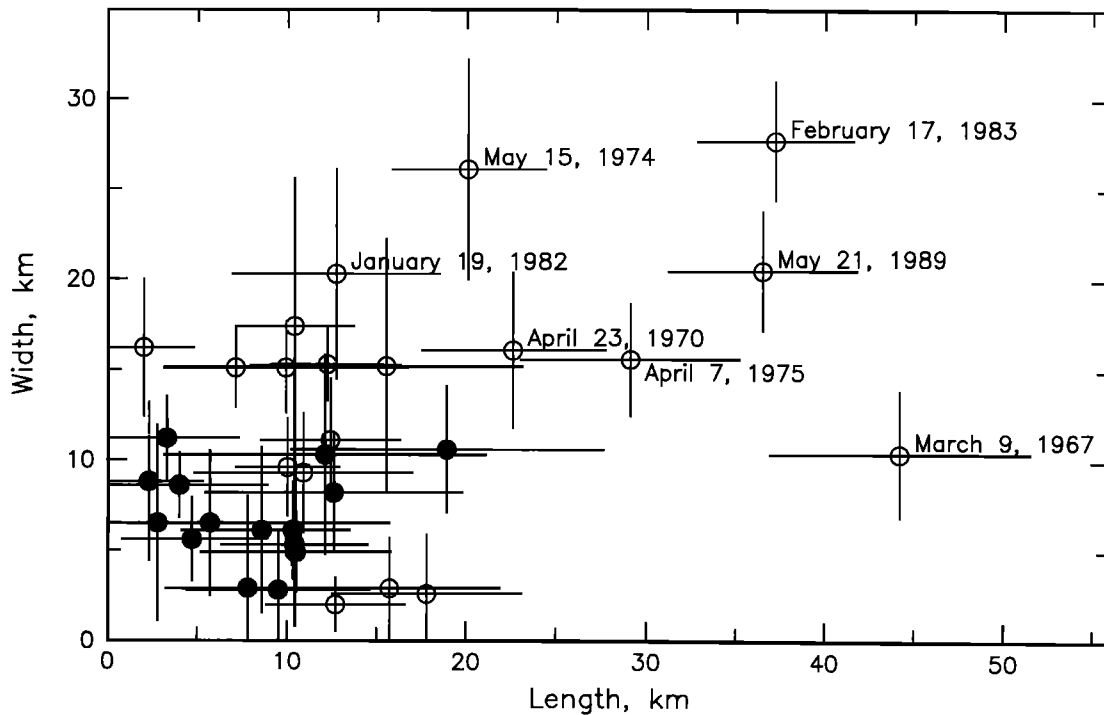


Fig. 20. Estimated width (cross-axis) and length (along axis) for 34 teleseismically located swarms, with  $1-\sigma$  error bars. Swarms which cannot be distinguished from a point source at the 99% confidence level (Table 1) are indicated by solid circles. Swarms with length or width greater than 20 km are labelled.

permit an accumulation of strain sufficient to produce an earthquake larger (judging from the observed seismicity) than about  $m_b = 5.0$ . The oceanic crust seems never to recover any significant seismic potential; larger oceanic intraplate earthquakes occur nearly always in the upper mantle [Bergman, 1986].

Observations of fresh and reactivated normal fault scarps in seismogenic rifting episodes at the Afar [Abdallah *et al.*,

1979] and Krafla [Sigurdsson, 1980] suggest that faults on both sides of the inner floor of the median valley may be active during a swarm. The observed across-axis extent of many of the relocated swarms in this study is consistent with such a view, but uncertainties in the absolute locations of the swarms are too large to allow us to verify such a relationship in most cases. In some cases, faults on opposite sides of the median valley may have been activated in swarms several

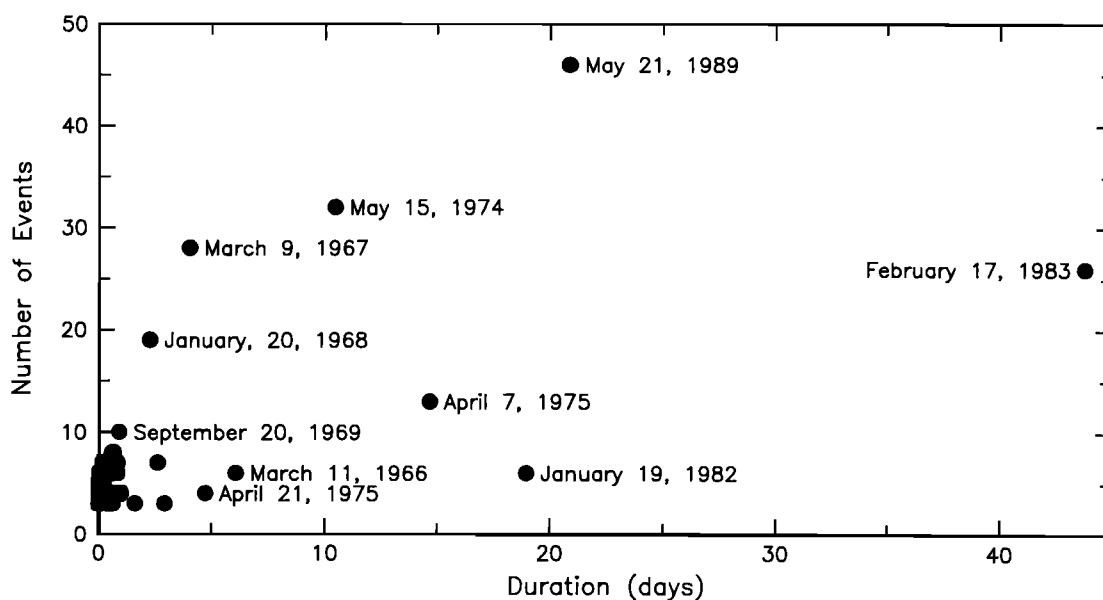


Fig. 21. Number of teleseismically detected earthquakes and duration for the 34 swarms listed in Table 1. The number includes events listed in the catalog of the ISC for which there were too few arrival time data to permit a reliable relocation. Swarms containing 10 or more events or lasting longer than 3 days are labelled.

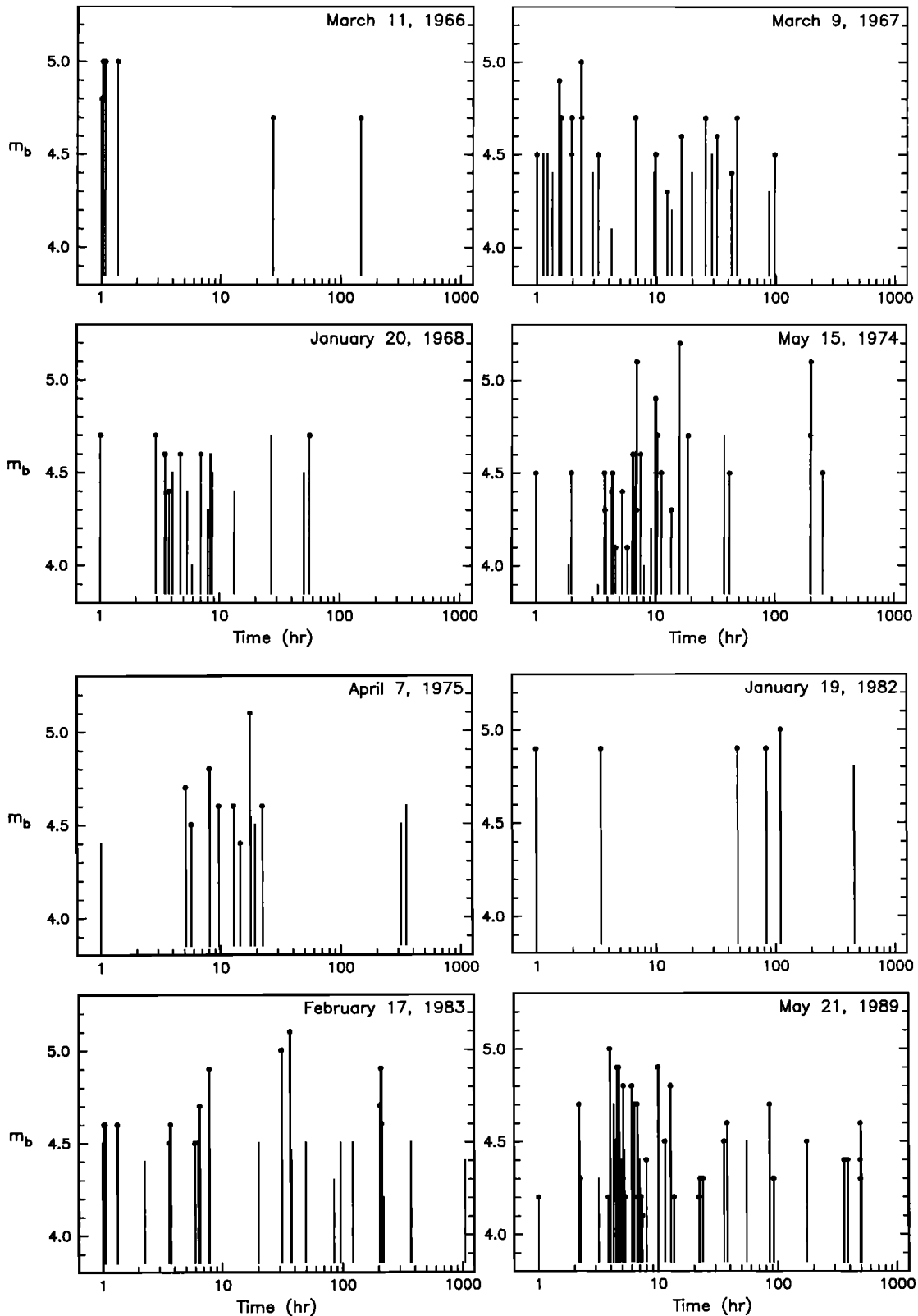


Fig. 22. Magnitude-time histories of eight swarms containing more than 10 events or lasting longer than 5 days. The time scale begins 1 hr before the first event in the swarm. Relocated events are indicated by a circle at the tip of the line.

years apart. From detailed microearthquake and Sea Beam mapping studies of the site of one of the swarms (June 28, 1977), *Toomey et al.* [1988] suggest that active extension on this part of the ridge is concentrated on the eastern side of

the inner floor. The relocated epicenters are generally consistent with this view, but one well-located event occurred  $\sim 7$  km WNW of the others (Figure 18), apparently on an en echelon fault strand.

There is still a need to account for the tendency of extensional faulting of the newly created oceanic crust to be expressed in earthquake swarms. The conditions leading to swarm-type microfracturing in laboratory specimens are heterogeneous material properties and a concentrated source of stress [Mogi, 1967]. Material heterogeneity at the ridge axis results from the high degree of order evident in the active faults which create the rift valley topography. Once past the initial episode of normal faulting at the foot of the inner median valley wall, the population of faults available for activation is remarkably uniform in orientation, spacing, and throw. We speculate that the dimensions and strengths of these faults are also quite uniform along any particular portion of the ridge. *Tapponnier and Francheteau* [1978] have suggested a mechanical model of slow-spreading, rifted ridges which predicts a stress concentration consistent with the activation of steeply-dipping inward-facing normal faults at the outer edge of the inner rift valley and in the rift mountains. At this location, the regional extensional stress responsible for normal faulting near the ridge axis is supplemented by a local stress field due to isostatic disequilibrium (resulting from necking of the lithosphere in the inner floor). Thus, the conditions necessary for swarm-type seismicity as a tectonic phenomena are likely present at rifted slow-spreading ridges, such as the MAR south of 60°N.

In planning marine geophysical surveys whose goal is to study volcanically-active portions of the mid-ocean ridge system, it would be quite helpful to be able to depend on a close correspondence between such activity and swarms of earthquakes large enough to be accurately located from teleseismic distances. Such a strategy, however, is problematic. A subset of the swarms considered here probably does have such an association, but we have been unable to identify any teleseismically-observable characteristic which would allow such a distinction to be made with confidence. Two opposing viewpoints thus remain viable. If extensional deformation of the ridge axis commonly occurs late in the spreading cycle, after the newly emplaced crust has cooled, strengthened, and accumulated significant extensional stress, the sites of many swarms, particularly those involving larger earthquakes, might be the least likely places to look for ongoing volcanism. However, if such deformation is the immediate precursor to a fresh episode of magmatism, then a site of repeated swarms would be a strong candidate among locations at which the volcanic phase of a slow spreading ridge segment might be clearly observed. The clearest path to a resolution of this issue lies in detailed geophysical and geological surveys of the sites of one or more recent swarms.

#### CONCLUSIONS

Teleseismically detected earthquake swarms on the mid-ocean ridge system have few features in common with swarms directly associated with active magmatism in terrestrial volcanic rift zones such as Hawaii and Iceland. The possibility that a subset of mid-ocean ridge swarms has such a relationship to a current episode of eruptive activity on the Mid-Atlantic Ridge cannot be excluded, but none of the 34 swarms studied is conspicuously attractive for such a role. Seismicity directly associated with volcanic activity on the mid-ocean ridge system probably occurs, with rare exceptions, at magnitudes below the detection threshold of current global seismic networks.

We conclude, therefore, that virtually all teleseismically located seismicity on slowly spreading segments of the mid-ocean ridge system, including swarms, is diagnostic of extensional tectonic activity and the development of the topographic relief of the median valley. The zone over which significant seismogenic extensional deformation occurs on the northern Mid-Atlantic Ridge is typically 10–20 km in width. The largest normal-faulting earthquakes on mid-ocean ridges may occur as members of swarms, in main-shock-aftershock sequences, or in isolation. We suggest that the largest earthquakes ( $m_b > 5.4$ ) usually occur at the main boundary faults of the inner floor of the median valley, while smaller events may occur within the terraces between the inner and outer rift walls, to maximum distances of 10–15 km from the axis of accretion. The tendency for mid-ocean ridge earthquakes to occur in swarms is speculatively attributed to the combined influence of material heterogeneity (from the high degree of order in the dimensions, orientations, spacings, and mechanical properties of the normal faults which create the ridge crest topography) and concentrations of stress arising from the normal mechanical evolution of newly emplaced lithosphere.

#### APPENDIX: RELOCATIONS OF INDIVIDUAL SWARMS

We review features of the individual swarms and the relocation analysis which are relevant to discussion of the characteristic dimensions of swarms and their tectonic significance. The swarms are grouped for discussion as in Table 1 and are identified by the date of the earliest event in each group. Individual earthquakes are identified by a code made up of the date and origin time (see Table A1) or an event number. The event numbers are also used in the figures showing cluster vectors; they are assigned to the events in chronological order in the swarms as grouped below and in Table 1.

*June 10, 1971, April 11, 1977, January 18, 1983, and May 21, 1989*

The epicentroids of these swarms and the local bathymetry are shown in Figure 1. The cluster vectors of the individual events are shown in Figure 6a. The 1971, 1977, and 1983 swarms occurred in a common source region approximately 20 km across. The 1977 swarm is elongated along the strike of the axis, but the 1983 swarm is elongated across the axis. A large fraction of the seismicity of the 1989 swarm was concentrated in a roughly circular pattern, about 10 km across, at the southern end of the cluster (Figure 6b). For 890522.0202 (#16,  $m_b = 5.0$ ), the largest event in the 1989 swarm, *Dziewonski et al.* [1989] report a centroid-moment tensor (CMT) solution characterized by right-lateral strike-slip faulting on a nodal plane striking at 052°. Further analysis, however, indicates that the waveform data, which have very poor signal-to-noise ratios, cannot reliably distinguish between such a mechanism and a steeply-dipping normal fault mechanism with nodal planes subparallel to the strike of the ridge (G. Zwart, personal communication, 1989). Event #16 occurred at the southernmost edge of the cluster.

*November 3, 1965, September 20, 1969, and February 17, 1983*

The epicentroids of these swarms and the local bathymetry are shown in Figure 1. The cluster vectors of the

individual events are shown in Figure 7. The sites of the 1965 and 1969 swarms coincide. The source mechanisms for several events in these swarms are known. *Huang et al.* [1986] studied 690920.0508 (#9,  $m_b = 5.6$ ), finding a normal-faulting mechanism with nodal planes striking  $023^\circ$  and  $035^\circ$ . All the events in the 1965 and 1969 swarms, with the exception of 690920.0113 (#7,  $m_b = 5.2$ ), could have occurred on a single fault with a strike of  $\sim 030^\circ$ . *Dziewonski et al.* [1988] report CMT solutions for 830217.1209 (#18,  $m_b = 4.9$ ) and 830218.1724 (#20,  $m_b = 5.1$ ); both are characterized by normal faulting, but with a substantial strike-slip component. The strikes of the nodal planes are  $016^\circ/049^\circ$  and  $018^\circ/068^\circ$ , respectively. These events could have both occurred about 10 km apart on a fault striking at  $\sim 015^\circ$ . In estimating the cross-axis extent of the 1983 swarm, it is tempting to exclude events 10 and 16 as mislocated (in which case the width is 11 km instead of 28 km), but both events are located with over 20 arrival times and the resolution of their locations in the cross-axis direction is good.

*September 28, 1970, January 26, 1977,  
and August 3, 1984*

The epicentroids for these swarms and the local bathymetry are shown in Figure 1. The cluster vectors of the individual events are shown in Figure 8. The 1977 and 1984 swarms occurred in close proximity. They form a pattern of ridge-parallel linear trends separated by about 10 km in the cross-axis direction. *Dziewonski et al.* [1985] report a CMT solution for 840803.0120 (#9,  $m_b = 5.1$ ) with a mechanism combining strike-slip and normal faulting. The nodal planes strike at  $018^\circ$  and  $078^\circ$ . The first nodal plane is close to the strike of the ridge ( $\sim 025^\circ$ ), but the second is close to the trend of most of the epicenters in the 1984 swarm (e.g., events #7, 9, 10, and 11).

*March 9, 1967, and April 23, 1970*

The epicentroids for these swarms and the local bathymetry are shown in Figure 2. The cluster vectors of the individual events are shown in Figure 9. The 1967 swarm may have been much more intense than our list of events indicates: the ISC catalog lists at least 25 events which were located primarily by the Large Aperture Seismic Array. Very few stations reported any arrival times for these events, however, and we have not included them in our study. *Tréhu et al.* [1981] conducted a moment-tensor inversion for the source mechanism of 700424.0123 (#20,  $m_b = 5.3$ ) using Rayleigh waves. The mechanism is a normal fault with the T-axis perpendicular to the ridge. The 1967 swarm contains an unusually large number of outliers on both sides of the main pattern of seismicity, but the locations of many of them are rather uncertain. The 1970 swarm also contains one conspicuous outlier (#23). These swarms occur where the overall strike of the Reykjanes Ridge abruptly changes by nearly  $30^\circ$  and the high level of off-axis seismicity, if it is real, may reflect a stress concentration in young lithosphere resulting from this change in trend. The length and width of the 1967 swarm were estimated from events 11 and 14, and 2 and 6, respectively, ignoring the outliers. There is a strong likelihood that we have underestimated the width of this swarm. Event #23 was not used to estimate the dimensions of the 1970 swarm.

*September 25, 1965, April 3, 1972,  
March 23, 1974, and July 31, 1984*

The epicentroids of these swarms are shown with the local bathymetry in Figure 2; the cluster vectors of the individual events are shown in Figure 10. The third event in the 1972 swarm (#6) occurred three days after the second and is much smaller than the first two events. *Einarsson* [1979] reported identical first-motion mechanisms for 720403.1852 (#4,  $m_b = 5.3$ ) and 720403.2036 (#5,  $m_b = 5.1$ ): a normal fault with nonorthogonal nodal planes striking at  $350^\circ$ – $360^\circ$ . *Tréhu et al.* [1981] performed body waveform modelling and moment tensor inversion with Rayleigh wave data for #5 to determine a normal faulting mechanism with both nodal planes striking  $004^\circ$ ; the nonorthogonal nodal planes in the first motion solution are the result of difficulty in picking the correct first motion for very shallow dip-slip earthquakes. Event #4 has nearly identical waveforms and probably a very similar mechanism. The CMT solution [*Dziewonski et al.*, 1985] for 840731.1210 (#10,  $m_b = 5.0$ ) has a normal faulting mechanism with nodal planes striking at  $007^\circ$  and  $018^\circ$ . The 1965, 1972, and 1984 swarms all lie within a well-defined north-south trending median valley, but the 1974 swarm apparently occurred within the western rift mountains. There is a strong suggestion that the 1965 and 1984 swarms occurred along opposite sides of the median valley, with a cross-axis separation of about 7–8 km.

*November 10, 1967, May 13, 1972,  
April 12, 1975, and September 1, 1979*

The epicentroids of these swarms are shown with the local bathymetry in Figure 3; the cluster vectors of the individual events are shown in Figure 11. We found that one event located by the ISC (790901.1220,  $m_b = 4.6$ ) with an unusually large standard error (4.7 s) actually consists of two events occurring about 9 s apart. Of the arrival times associated to one event by the ISC, 45 correspond to event #10 and 26 to #11. The two events are separated by about 8 km along the eastern edge of the swarm.

*April 7, 1975, and September 10, 1979*

The epicentroids of these swarms are shown with the local bathymetry in Figure 3; the cluster vectors of the individual events are shown in Figure 12. These two swarms appear to be immediately adjacent to one another. One clear outlier (#11,  $m_b = 4.4$ ) has only 14 arrival times and is probably mislocated; it is not used to estimate the extent of the 1979 swarm.

*January 20, 1968, June 10, 1975,  
and March 9, 1984*

The epicentroids of these swarms are shown with the local bathymetry in Figure 3; the cluster vectors of the individual events are shown in Figure 13. The 1975 and 1984 swarms coincide, and both have a strong elongation oriented NW–SE. Considering that the absolute locations are probably biased to the north by  $\sim 10$  km, the 1975 and 1984 swarms appear to have occurred in the vicinity of the Kurchatov Fracture Zone, immediately north of the Azores triple junction. *Searle and Laughton* [1977] found no morphologic evidence to justify a description of the ridge offset as a transform fault, however, concluding that it is best characterized as a zone of oblique spreading oriented at  $055^\circ$ . The

TABLE A1. Epicentral Data From Relocation

Date	Origin Time	Latitude, °N	Longitude, °W	$m_b$	$N^*$
Sept. 25, 1965	1011:28.2 ± 0.34	54.02 ± 0.087	35.33 ± 0.061	4.4	16
Sept. 25, 1965	2010:06.0 ± 0.13	54.02 ± 0.040	35.25 ± 0.022	4.9	51
Sept. 26, 1965	1003:17.7 ± 0.13	54.04 ± 0.039	35.23 ± 0.022	4.7	49
Nov. 3, 1965	0753:11.6 ± 0.16	58.15 ± 0.055	32.12 ± 0.039	4.6	28
Nov. 3, 1965	0757:33.4 ± 0.21	58.12 ± 0.065	32.14 ± 0.042	4.7	15
Nov. 3, 1965	0833:51.4 ± 0.12	58.26 ± 0.037	32.17 ± 0.029	4.7	38
March 11, 1966	2313:26.8 ± 0.16	28.33 ± 0.025	43.88 ± 0.030	4.8	24
March 11, 1966	2315:42.1 ± 0.10	28.32 ± 0.020	43.87 ± 0.014	5.0	57
March 11, 1966	2318:49.4 ± 0.13	28.34 ± 0.024	43.86 ± 0.021	5.0	26
March 11, 1966	2336:41.5 ± 0.09	28.30 ± 0.019	43.89 ± 0.014	5.0	63
March 13, 1966	0136:33.9 ± 0.11	28.31 ± 0.022	43.86 ± 0.018	4.7	38
March 18, 1966	0110:25.6 ± 0.13	28.39 ± 0.024	43.86 ± 0.019	4.7	26
Feb. 17, 1967	1006:45.6 ± 0.11	28.84 ± 0.024	43.47 ± 0.023	4.8	29
Feb. 17, 1967	1557:47.5 ± 0.12	28.87 ± 0.022	43.45 ± 0.024	4.7	31
Feb. 18, 1967	0031:47.3 ± 0.09	28.90 ± 0.019	43.39 ± 0.016	5.2	47
March 9, 1967	2002:42.5 ± 0.30	55.96 ± 0.042	34.62 ± 0.061	4.5	22
March 9, 1967	2034:47.2 ± 0.15	56.11 ± 0.029	34.62 ± 0.032	4.9	39
March 9, 1967	2038:35.5 ± 0.48	56.05 ± 0.048	34.65 ± 0.112	4.7	20
March 9, 1967	2059:42.3 ± 0.14	56.05 ± 0.027	34.53 ± 0.035	4.5	25
March 9, 1967	2100:53.7 ± 0.20	56.31 ± 0.048	34.34 ± 0.043	4.7	12
March 9, 1967	2122:48.1 ± 0.09	56.06 ± 0.024	34.48 ± 0.021	5.0	48
March 9, 1967	2124:53.7 ± 0.31	56.02 ± 0.064	35.13 ± 0.048	4.7	19
March 9, 1967	2217:59.7 ± 0.44	55.97 ± 0.042	34.56 ± 0.105	4.5	18
March 10, 1967	0143:54.9 ± 0.22	56.01 ± 0.029	34.73 ± 0.051	4.7	25
March 10, 1967	0454:55.2 ± 0.37	56.19 ± 0.066	35.07 ± 0.080	4.5	13
March 10, 1967	0721:50.4 ± 0.16	56.14 ± 0.042	34.56 ± 0.032	4.3	15
March 10, 1967	1114:37.2 ± 0.14	55.96 ± 0.036	34.62 ± 0.031	4.6	31
March 10, 1967	2046:33.8 ± 0.13	55.92 ± 0.028	34.75 ± 0.031	4.7	32
March 11, 1967	0305:25.4 ± 0.14	55.77 ± 0.036	34.83 ± 0.036	4.6	25
March 11, 1967	1334:26.6 ± 0.27	55.82 ± 0.049	34.50 ± 0.074	4.4	11
March 11, 1967	1815:15.4 ± 0.30	55.78 ± 0.046	34.36 ± 0.060	4.7	18
March 13, 1967	2050:29.4 ± 0.14	56.18 ± 0.033	35.06 ± 0.031	4.5	18
Nov. 10, 1967	0440:14.7 ± 0.12	45.04 ± 0.030	28.02 ± 0.021	4.7	36
Nov. 10, 1967	0512:01.1 ± 0.17	45.11 ± 0.036	28.13 ± 0.029	4.3	17
Nov. 10, 1967	0550:27.7 ± 0.18	44.93 ± 0.049	28.14 ± 0.026	4.7	17
Jan. 20, 1968	0627:39.8 ± 0.20	41.24 ± 0.040	29.38 ± 0.053	4.7	22
Jan. 20, 1968	0822:28.7 ± 0.13	41.24 ± 0.034	29.40 ± 0.025	4.7	30
Jan. 20, 1968	0857:44.5 ± 0.19	41.37 ± 0.037	29.35 ± 0.035	4.6	25
Jan. 20, 1968	0914:21.4 ± 0.24	41.25 ± 0.057	29.23 ± 0.032	4.4	9
Jan. 20, 1968	1010:48.1 ± 0.22	41.32 ± 0.055	29.41 ± 0.064	4.6	9
Jan. 20, 1968	1226:05.9 ± 0.17	41.37 ± 0.044	29.25 ± 0.034	4.6	13
Jan. 22, 1968	1321:33.1 ± 0.19	41.31 ± 0.044	29.31 ± 0.021	4.7	30
Sept. 20, 1969	0020:49.6 ± 0.18	58.19 ± 0.048	32.25 ± 0.058	4.5	11
Sept. 20, 1969	0056:51.2 ± 0.10	58.22 ± 0.023	32.18 ± 0.023	4.9	59
Sept. 20, 1969	0107:38.1 ± 0.09	58.22 ± 0.023	32.09 ± 0.021	5.0	78
Sept. 20, 1969	0113:04.0 ± 0.09	58.11 ± 0.021	32.03 ± 0.023	5.2	60
Sept. 20, 1969	0324:26.8 ± 0.28	58.13 ± 0.047	32.11 ± 0.063	4.5	14
Sept. 20, 1969	0508:56.3 ± 0.07	58.28 ± 0.018	32.12 ± 0.017	5.6	117
April 23, 1970	1543:38.9 ± 0.15	55.56 ± 0.033	35.05 ± 0.033	4.6	29
April 24, 1970	0121:16.2 ± 0.20	55.63 ± 0.037	35.26 ± 0.034	4.6	31
April 24, 1970	0123:14.9 ± 0.09	55.65 ± 0.019	34.99 ± 0.019	5.3	109
April 24, 1970	0147:13.4 ± 0.11	55.53 ± 0.023	35.07 ± 0.025	4.7	64
April 24, 1970	0151:19.8 ± 0.19	55.52 ± 0.038	35.31 ± 0.031	4.7	36
April 24, 1970	0529:00.9 ± 0.23	55.25 ± 0.042	34.77 ± 0.052	4.5	13
April 26, 1970	0639:50.6 ± 0.09	55.51 ± 0.019	35.11 ± 0.021	4.9	100
Sept. 28, 1970	1139:08.1 ± 0.11	57.17 ± 0.030	33.27 ± 0.027	4.5	46
Sept. 28, 1970	2349:31.1 ± 0.10	57.18 ± 0.028	33.37 ± 0.024	4.6	55
Sept. 28, 1970	2357:03.3 ± 0.10	57.20 ± 0.028	33.29 ± 0.025	4.8	50
June 10, 1971	1854:04.2 ± 0.14	59.49 ± 0.026	30.41 ± 0.034	4.4	17
June 10, 1971	1902:41.3 ± 0.12	59.50 ± 0.025	30.35 ± 0.028	4.7	29
June 10, 1971	2132:38.1 ± 0.10	59.37 ± 0.021	30.38 ± 0.022	5.0	40
June 11, 1971	0641:31.8 ± 0.16	59.44 ± 0.034	30.24 ± 0.036	4.5	10
April 3, 1972	1852:58.8 ± 0.07	54.24 ± 0.018	35.06 ± 0.014	5.3	169
April 3, 1972	2036:21.5 ± 0.07	54.29 ± 0.017	35.11 ± 0.014	5.1	175
April 6, 1972	1716:02.8 ± 0.17	54.27 ± 0.056	35.16 ± 0.055	...	13
May 13, 1972	1506:38.3 ± 0.12	45.17 ± 0.023	28.08 ± 0.016	4.6	53
May 13, 1972	1637:12.9 ± 0.17	45.09 ± 0.033	28.17 ± 0.018	4.7	40
May 13, 1972	1640:21.4 ± 0.10	45.12 ± 0.021	28.09 ± 0.014	4.9	76
March 23, 1974	0705:03.7 ± 0.11	53.87 ± 0.035	35.53 ± 0.022	4.6	33
March 23, 1974	0709:02.6 ± 0.08	53.90 ± 0.020	35.39 ± 0.016	4.8	83
March 23, 1974	0719:13.9 ± 0.07	53.90 ± 0.018	35.45 ± 0.015	5.0	120
May 15, 1974	0437:39.2 ± 0.13	27.41 ± 0.023	44.28 ± 0.018	4.5	29

TABLE A1. (continued)

Date	Origin Time	Latitude, °N	Longitude, °W	$m_b$	$N^*$
May 15, 1974	0536:12.7 ± 0.09	27.42 ± 0.017	44.19 ± 0.014	4.5	49
May 15, 1974	0722:49.3 ± 0.14	27.44 ± 0.025	44.32 ± 0.020	4.5	23
May 15, 1974	0725:06.1 ± 0.23	27.40 ± 0.030	44.23 ± 0.044	4.3	8
May 15, 1974	0755:04.4 ± 0.21	27.44 ± 0.035	44.35 ± 0.043	4.4	8
May 15, 1974	0800:33.6 ± 0.14	27.40 ± 0.024	44.16 ± 0.026	4.5	12
May 15, 1974	0816:57.1 ± 0.23	27.13 ± 0.029	44.23 ± 0.041	4.1	11
May 15, 1974	0854:54.2 ± 0.17	27.43 ± 0.026	44.32 ± 0.024	4.4	23
May 15, 1974	0927:33.8 ± 0.22	27.34 ± 0.041	44.17 ± 0.027	4.1	10
May 15, 1974	1005:46.7 ± 0.13	27.42 ± 0.019	44.28 ± 0.026	4.6	24
May 15, 1974	1020:06.6 ± 0.13	27.36 ± 0.024	44.26 ± 0.024	4.4	17
May 15, 1974	1033:19.7 ± 0.18	27.39 ± 0.027	44.25 ± 0.029	4.3	15
May 15, 1974	1033:58.4 ± 0.09	27.38 ± 0.018	44.21 ± 0.015	5.1	58
May 15, 1974	1108:06.6 ± 0.14	27.30 ± 0.024	44.37 ± 0.019	4.6	29
May 15, 1974	1337:10.9 ± 0.08	27.43 ± 0.014	44.27 ± 0.012	4.9	94
May 15, 1974	1344:10.3 ± 0.09	27.39 ± 0.017	44.31 ± 0.015	4.5	43
May 15, 1974	1359:14.9 ± 0.14	27.33 ± 0.026	44.34 ± 0.014	4.7	54
May 15, 1974	1452:04.9 ± 0.15	27.35 ± 0.026	44.24 ± 0.021	4.5	21
May 15, 1974	1713:41.3 ± 0.23	27.51 ± 0.045	44.18 ± 0.020	4.3	20
May 15, 1974	1929:31.2 ± 0.11	27.30 ± 0.020	44.35 ± 0.015	5.2	59
May 15, 1974	2221:39.1 ± 0.08	27.38 ± 0.015	44.26 ± 0.013	4.7	71
May 16, 1974	2123:48.4 ± 0.22	27.41 ± 0.040	44.31 ± 0.023	4.5	20
May 23, 1974	0922:59.7 ± 0.10	27.34 ± 0.018	44.31 ± 0.019	4.7	23
May 23, 1974	1108:24.4 ± 0.07	27.32 ± 0.013	44.40 ± 0.011	5.1	107
May 25, 1974	1546:00.5 ± 0.15	27.41 ± 0.025	44.43 ± 0.024	4.5	25
April 7, 1975	2251:32.6 ± 0.14	42.60 ± 0.036	29.44 ± 0.040	4.7	15
April 7, 1975	2325:36.9 ± 0.20	42.41 ± 0.041	29.42 ± 0.023	4.5	17
April 8, 1975	0151:29.3 ± 0.10	42.64 ± 0.020	29.31 ± 0.014	4.8	95
April 8, 1975	0328:22.1 ± 0.17	42.57 ± 0.035	29.42 ± 0.022	4.6	21
April 8, 1975	0643:26.4 ± 0.14	42.53 ± 0.032	29.49 ± 0.022	4.6	23
April 8, 1975	0825:57.2 ± 0.26	42.68 ± 0.055	29.49 ± 0.023	4.4	17
April 8, 1975	1136:53.3 ± 0.09	42.68 ± 0.019	29.42 ± 0.013	5.1	105
April 8, 1975	1616:33.6 ± 0.20	42.59 ± 0.043	29.50 ± 0.040	4.6	17
April 21, 1975	0612:21.9 ± 0.21	45.43 ± 0.042	27.97 ± 0.024	4.3	18
April 21, 1975	0614:31.9 ± 0.10	45.35 ± 0.020	27.97 ± 0.013	4.9	82
April 21, 1975	1914:56.6 ± 0.18	45.49 ± 0.039	27.91 ± 0.018	4.7	50
June 10, 1975	0604:48.0 ± 0.11	40.74 ± 0.023	29.42 ± 0.016	5.0	80
June 10, 1975	0728:33.3 ± 0.14	40.69 ± 0.031	29.37 ± 0.019	4.6	47
June 10, 1975	0852:20.2 ± 0.13	40.75 ± 0.028	29.45 ± 0.017	4.7	65
Jan. 26, 1977	2329:13.2 ± 0.16	57.61 ± 0.041	33.06 ± 0.055	4.4	17
Jan. 27, 1977	0025:31.5 ± 0.15	57.60 ± 0.044	32.94 ± 0.054	4.6	17
Jan. 28, 1977	1411:30.4 ± 0.11	57.72 ± 0.031	32.99 ± 0.023	4.9	49
April 11, 1977	2214:26.4 ± 0.23	59.49 ± 0.032	30.09 ± 0.045	3.9	10
April 11, 1977	2226:28.8 ± 0.10	59.45 ± 0.021	30.16 ± 0.025	4.5	50
April 11, 1977	2244:41.6 ± 0.11	59.50 ± 0.021	30.13 ± 0.024	4.6	41
April 11, 1977	2320:41.7 ± 0.09	59.36 ± 0.016	30.27 ± 0.022	4.6	49
June 28, 1977	1538:36.7 ± 0.07	22.66 ± 0.014	45.07 ± 0.009	5.3	199
June 28, 1977	1618:14.6 ± 0.06	22.70 ± 0.012	45.12 ± 0.008	5.5	252
June 28, 1977	1856:47.6 ± 0.11	22.64 ± 0.021	45.04 ± 0.016	4.6	38
June 28, 1977	1918:34.9 ± 0.06	22.64 ± 0.011	45.07 ± 0.008	5.9	262
June 28, 1977	1935:01.4 ± 0.10	22.60 ± 0.018	45.10 ± 0.011	5.0	104
Sept. 1, 1979	1220:53.9 ± 0.19	44.93 ± 0.041	28.05 ± 0.017	4.6	39
Sept. 1, 1979	1221:02.7 ± 0.16	44.99 ± 0.043	28.00 ± 0.022	4.6	23
Sept. 1, 1979	1303:42.0 ± 0.12	44.95 ± 0.027	28.04 ± 0.013	4.8	87
Sept. 1, 1979	1320:29.7 ± 0.11	44.99 ± 0.023	28.12 ± 0.012	4.8	89
Sept. 1, 1979	1327:47.9 ± 0.09	44.90 ± 0.020	28.06 ± 0.012	4.9	94
Sept. 1, 1979	1404:26.9 ± 0.15	45.00 ± 0.033	28.08 ± 0.014	4.6	59
Sept. 10, 1979	0544:43.7 ± 0.17	42.74 ± 0.033	29.36 ± 0.021	4.1	27
Sept. 10, 1979	0632:07.0 ± 0.13	42.75 ± 0.028	29.27 ± 0.013	4.6	85
Sept. 10, 1979	0729:58.0 ± 0.24	42.54 ± 0.060	28.99 ± 0.023	4.4	14
Sept. 10, 1979	0802:57.3 ± 0.18	42.73 ± 0.038	29.35 ± 0.019	4.4	31
Sept. 10, 1979	0904:49.4 ± 0.18	42.79 ± 0.042	29.35 ± 0.019	4.4	23
Sept. 10, 1979	1100:07.3 ± 0.18	42.83 ± 0.039	29.43 ± 0.021	4.5	32
Sept. 11, 1979	0152:29.5 ± 0.11	42.79 ± 0.024	29.27 ± 0.012	4.9	105
Jan. 19, 1982	0409:25.9 ± 0.11	21.56 ± 0.020	45.36 ± 0.015	4.9	47
Jan. 19, 1982	0638:14.5 ± 0.18	21.55 ± 0.026	45.32 ± 0.030	4.9	22
Jan. 21, 1982	0334:09.0 ± 0.11	21.53 ± 0.020	45.42 ± 0.013	4.9	84
Jan. 22, 1982	1513:34.7 ± 0.14	21.52 ± 0.024	45.52 ± 0.018	4.9	38
Jan. 23, 1982	1755:49.4 ± 0.14	21.63 ± 0.025	45.47 ± 0.015	5.0	67
Jan. 18, 1983	0828:11.9 ± 0.11	59.39 ± 0.023	30.33 ± 0.031	4.6	28
Jan. 18, 1983	0834:49.3 ± 0.09	59.34 ± 0.021	30.26 ± 0.021	4.7	48
Jan. 18, 1983	0946:43.8 ± 0.09	59.40 ± 0.021	30.43 ± 0.023	4.8	44
Feb. 17, 1983	0519:13.7 ± 0.12	58.63 ± 0.045	31.79 ± 0.032	4.6	21
Feb. 17, 1983	0520:27.4 ± 0.09	58.61 ± 0.027	31.66 ± 0.023	4.6	35

TABLE A1. (continued)

Date	Origin Time	Latitude, °N	Longitude, °W	$m_b$	$N^*$
Feb. 17, 1983	0537:15.4 ± 0.12	58.51 ± 0.033	31.66 ± 0.025	4.6	24
Feb. 17, 1983	0753:05.2 ± 0.15	58.61 ± 0.037	31.63 ± 0.029	4.5	18
Feb. 17, 1983	0801:12.0 ± 0.14	58.71 ± 0.029	31.39 ± 0.032	4.6	36
Feb. 17, 1983	1015:17.1 ± 0.18	58.67 ± 0.039	31.38 ± 0.045	4.5	24
Feb. 17, 1983	1036:38.1 ± 0.14	58.38 ± 0.037	31.54 ± 0.034	4.5	26
Feb. 17, 1983	1049:40.3 ± 0.09	58.41 ± 0.028	31.70 ± 0.024	4.7	38
Feb. 17, 1983	1209:39.5 ± 0.06	58.46 ± 0.016	31.76 ± 0.015	4.9	152
Feb. 18, 1983	1151:30.0 ± 0.06	58.41 ± 0.016	31.70 ± 0.015	5.0	123
Feb. 18, 1983	1724:18.1 ± 0.07	58.55 ± 0.016	31.72 ± 0.016	5.1	160
Feb. 25, 1983	1832:16.6 ± 0.11	58.65 ± 0.023	31.49 ± 0.022	4.7	71
Feb. 25, 1983	2350:27.5 ± 0.09	58.46 ± 0.028	31.67 ± 0.022	4.9	56
Feb. 26, 1983	0122:23.7 ± 0.08	58.68 ± 0.031	31.47 ± 0.023	4.6	51
Jan. 15, 1984	0702:12.9 ± 0.09	28.88 ± 0.018	43.40 ± 0.015	4.9	55
Jan. 15, 1984	0714:13.6 ± 0.09	28.83 ± 0.017	43.51 ± 0.015	5.2	46
Jan. 15, 1984	0735:12.0 ± 0.10	28.86 ± 0.021	43.45 ± 0.021	4.9	28
March 9, 1984	1003:08.6 ± 0.15	40.77 ± 0.031	29.48 ± 0.019	4.7	66
March 9, 1984	1540:52.0 ± 0.14	40.65 ± 0.025	29.38 ± 0.020	4.9	86
March 9, 1984	1908:22.6 ± 0.12	40.67 ± 0.024	29.41 ± 0.018	4.9	96
March 15, 1984	2209:48.6 ± 0.16	28.49 ± 0.030	43.75 ± 0.018	4.5	24
March 15, 1984	2318:21.5 ± 0.11	28.44 ± 0.020	43.71 ± 0.015	4.9	63
March 16, 1984	0043:20.3 ± 0.10	28.41 ± 0.018	43.78 ± 0.015	5.0	53
July 31, 1984	1210:56.5 ± 0.08	54.04 ± 0.021	35.15 ± 0.015	5.0	125
July 31, 1984	1220:39.3 ± 0.09	53.99 ± 0.025	35.15 ± 0.016	4.9	92
July 31, 1984	1226:05.1 ± 0.10	53.92 ± 0.028	35.13 ± 0.019	4.8	71
Aug. 3, 1984	0109:12.4 ± 0.07	57.66 ± 0.021	32.74 ± 0.018	4.8	122
Aug. 3, 1984	0119:32.4 ± 0.14	57.70 ± 0.040	32.99 ± 0.035	4.4	30
Aug. 3, 1984	0121:01.6 ± 0.07	57.63 ± 0.019	32.82 ± 0.017	5.1	141
Aug. 3, 1984	0406:46.8 ± 0.11	57.63 ± 0.029	32.80 ± 0.028	4.4	32
Aug. 3, 1984	2054:49.5 ± 0.07	57.62 ± 0.019	32.86 ± 0.018	4.8	132
Jan. 18, 1985	2313:01.8 ± 0.10	29.98 ± 0.017	42.80 ± 0.019	5.0	77
Jan. 18, 1985	2316:07.8 ± 0.15	29.93 ± 0.025	42.70 ± 0.035	4.9	11
Jan. 18, 1985	2326:03.6 ± 0.10	29.88 ± 0.019	42.63 ± 0.021	4.9	60
Jan. 18, 1985	2355:14.2 ± 0.26	29.99 ± 0.035	42.79 ± 0.058	4.7	7
Jan. 19, 1985	0006:10.5 ± 0.10	29.99 ± 0.018	42.76 ± 0.019	4.9	56
Jan. 19, 1985	1237:16.2 ± 0.09	29.90 ± 0.017	42.68 ± 0.018	5.0	92
July 13, 1985	1854:14.8 ± 0.10	25.93 ± 0.015	45.01 ± 0.019	5.0	162
July 13, 1985	1900:20.5 ± 0.15	25.89 ± 0.024	45.02 ± 0.032	4.6	12
July 13, 1985	1907:03.1 ± 0.26	25.94 ± 0.029	45.12 ± 0.057	4.4	7
July 13, 1985	1909:20.0 ± 0.10	25.96 ± 0.015	45.02 ± 0.019	5.0	162
July 13, 1985	1939:17.1 ± 0.14	25.89 ± 0.023	45.01 ± 0.028	4.5	16
May 21, 1989	2303:51.1 ± 0.16	59.93 ± 0.023	29.85 ± 0.039	4.2	16
May 22, 1989	0014:16.4 ± 0.08	59.87 ± 0.017	29.74 ± 0.020	4.7	62
May 22, 1989	0017:02.1 ± 0.24	59.83 ± 0.030	29.78 ± 0.053	4.3	8
May 22, 1989	0152:22.7 ± 0.21	59.95 ± 0.021	29.59 ± 0.047	4.2	19
May 22, 1989	0202:06.0 ± 0.08	59.74 ± 0.021	29.74 ± 0.023	5.0	78
May 22, 1989	0229:16.8 ± 0.13	59.96 ± 0.023	29.67 ± 0.032	4.5	37
May 22, 1989	0236:47.7 ± 0.16	59.83 ± 0.017	29.63 ± 0.036	4.4	38
May 22, 1989	0238:39.9 ± 0.09	59.86 ± 0.017	29.69 ± 0.022	4.9	66
May 22, 1989	0246:39.0 ± 0.08	59.86 ± 0.019	29.58 ± 0.021	4.9	80
May 22, 1989	0309:05.9 ± 0.12	59.81 ± 0.021	29.73 ± 0.030	4.3	30
May 22, 1989	0312:57.1 ± 0.08	59.84 ± 0.018	29.64 ± 0.020	4.8	58
May 22, 1989	0320:56.4 ± 0.19	59.81 ± 0.021	29.73 ± 0.043	4.2	20
May 22, 1989	0406:24.5 ± 0.09	59.99 ± 0.019	29.60 ± 0.026	4.8	54
May 22, 1989	0420:55.9 ± 0.09	59.86 ± 0.019	29.73 ± 0.022	4.7	51
May 22, 1989	0442:43.1 ± 0.20	59.97 ± 0.031	29.84 ± 0.050	4.2	11
May 22, 1989	0445:36.8 ± 0.10	59.84 ± 0.020	29.69 ± 0.026	4.7	53
May 22, 1989	0515:50.3 ± 0.21	59.82 ± 0.030	29.62 ± 0.046	4.2	12
May 22, 1989	0525:21.5 ± 0.16	59.93 ± 0.022	29.65 ± 0.035	4.1	19
May 22, 1989	0603:40.7 ± 0.10	59.75 ± 0.020	29.75 ± 0.024	4.4	37
May 22, 1989	0807:37.0 ± 0.07	60.02 ± 0.018	29.62 ± 0.020	4.9	77
May 22, 1989	0928:02.4 ± 0.13	59.76 ± 0.021	29.80 ± 0.029	4.5	29
May 22, 1989	1050:32.1 ± 0.10	59.79 ± 0.023	29.78 ± 0.027	4.8	40
May 22, 1989	1135:06.6 ± 0.17	59.83 ± 0.027	29.65 ± 0.041	4.2	15
May 22, 1989	2000:31.2 ± 0.23	59.78 ± 0.031	29.70 ± 0.054	4.2	16
May 22, 1989	2031:52.1 ± 0.16	59.82 ± 0.026	29.68 ± 0.039	4.3	24
May 22, 1989	2145:39.0 ± 0.21	59.84 ± 0.022	29.77 ± 0.048	4.3	13
May 23, 1989	0947:25.8 ± 0.11	59.86 ± 0.033	29.71 ± 0.034	4.5	33
May 23, 1989	1211:19.4 ± 0.13	59.87 ± 0.034	29.69 ± 0.037	4.6	26
May 25, 1989	1143:49.1 ± 0.11	59.81 ± 0.024	29.62 ± 0.031	4.7	42
May 25, 1989	1901:40.1 ± 0.16	59.95 ± 0.028	29.66 ± 0.041	4.3	23
May 29, 1989	0555:45.2 ± 0.11	59.84 ± 0.021	29.64 ± 0.027	4.5	28
June 5, 1989	2221:19.7 ± 0.13	60.03 ± 0.023	29.50 ± 0.031	4.4	35

TABLE A1. (continued)

Date	Origin Time	Latitude, °N	Longitude, °W	$m_b$	$N^*$
June 7, 1989	0135:23.1 ± 0.27	60.02 ± 0.025	29.41 ± 0.058	4.4	11
June 11, 1989	1008:29.9 ± 0.09	59.78 ± 0.019	29.65 ± 0.023	4.4	38
June 11, 1989	1038:13.4 ± 0.19	59.82 ± 0.022	29.81 ± 0.046	4.3	15
June 11, 1989	1242:19.2 ± 0.14	59.80 ± 0.020	29.62 ± 0.034	4.3	27
June 11, 1989	1253:28.5 ± 0.26	59.78 ± 0.023	29.70 ± 0.058	4.6	10

Events listed in chronological order. Uncertainties are for cluster vectors, i.e., they are the uncertainties relative to the hypocentroid. See Table 1 for groupings used in relocation and uncertainty of hypocentroid. Depth fixed at 10 km for all relocations.

\*Number of stations used to calculate the cluster vector.

width and length of these two swarms were calculated relative to this direction. Relative to the regional trend of more typical ridge segments in this region, the estimated length and width of the 1975 swarm ( $5 \pm 5$  and  $8 \pm 2$  km, respectively) would be similar to the values given in Table 1, while the length and width of the 1984 swarm would be  $13 \pm 4$  and  $9 \pm 2$  km, respectively.

#### January 18, 1985

The epicentroid and the local bathymetry are shown in Figure 4. The cluster vectors of the individual events are shown in Figure 14. Events 850118.2316 (#2,  $m_b = 4.9$ ) and 850118.2355 (#4,  $m_b = 4.7$ ) were located with 11 and 7 arrival times, respectively, but their epicenters are consistent with the pattern defined by the better-located events. This swarm is located immediately to the south of the western end of the Atlantis Fracture Zone. To verify that this swarm, which is elongated in the approximate direction of the transform, is truly a swarm of ridge axis earthquakes, we relocated it with other earthquakes in the area, including events within the transform and to the north and south of the transform. Judging from the geometry of these relocated earthquakes, the 1985 swarm is located about 20 km south of the ridge-transform intersection.

#### March 11, 1966, February 17, 1967, January 15, 1984, and March 15, 1984

The epicentroids of these swarms and the local bathymetry are shown in Figure 4. The cluster vectors of the individual events are shown in Figure 15. The locations of the 1967 and January 1984 swarms coincide, while the 1966 and March 1984 swarms appear to be immediately adjacent to one another. There is a CMT solution [Dziewonski *et al.*, 1984] for 840115.0714 (#11,  $m_b = 5.2$ ), with a normal faulting mechanism and nodal planes striking at  $345^\circ$  and  $006^\circ$ . Neither plane is close to the trend of the median valley ( $035^\circ$ ).

#### May 15, 1974

The epicentroid for this large swarm and the local bathymetry are shown in Figure 4. The cluster vectors of the individual events are shown in Figure 16. The final three events (#23–25) in this swarm occurred one week after the main swarm (Figure 22). Events #7 ( $m_b = 4.1$ ) and #19 ( $m_b = 4.3$ ) are poorly located outliers; they were not used to estimate the extent of this swarm.

#### July 13, 1985

The epicentroid and the local bathymetry are shown in Figure 4. The cluster vectors of the individual events are

shown in Figure 17. Event 850713.1907 (#3,  $m_b = 4.4$ ) is located with only seven arrival times; it was not used to estimate the spatial extent of this swarm. There are CMT solutions [Dziewonski *et al.*, 1986] for 850713.1854 (#1,  $m_b = 5.0$ ) and 850713.1909 (#4,  $m_b = 5.0$ ), both characterized by normal faulting with nodal planes striking at  $001^\circ$  and  $032^\circ$ , and  $001^\circ$  and  $015^\circ$ , respectively. All five events could have occurred on a single fault with a strike of near  $0^\circ$ .

#### June 28, 1977

The epicentroid for this swarm and the local bathymetry are shown in Figure 5, while the cluster vectors of the individual events are shown in Figure 18. Four of the five events in this swarm have  $m_b \geq 5.0$ , and source mechanism studies have been conducted for three of them. Huang *et al.* [1986] studied 770628.1538 (#1,  $m_b = 5.3$ ) and 770628.1918 (#4,  $m_b = 5.9$ ) with a body waveform inversion method, obtaining normal faulting mechanisms with nodal planes striking at  $001^\circ$  and  $023^\circ$  for both events. CMT solutions for these two events [Dziewonski *et al.*, 1987] have nodal planes striking at  $005^\circ$  and  $048^\circ$ , and  $007^\circ$  and  $042^\circ$ , respectively. The CMT solution for 770628.1618 (#2,  $m_b = 5.5$ ) has nodal planes striking at  $027^\circ$  and  $059^\circ$ , but this result is probably less reliable because of interference from event #1. By matching the dominant period of water column reverberations in the long-period P waveforms, Huang *et al.* [1986] estimated the water depth at the sites of events #1 and #4 to be 4.0 and 3.5 km, respectively. These depths are in reasonable agreement with those expected from the bathymetry [e.g., Toomey *et al.*, 1988] and the locations in Table A1, but they suggest either that event #1 actually occurred slightly east of event #4, rather than at the same longitude as indicated in Figure 18, or that the epicentroid is mislocated to the north by about 5 km.

#### January 19, 1982

The epicentroid and the local bathymetry are shown in Figure 5. The cluster vectors of the individual events are shown in Figure 19. The temporal pattern of this swarm is quite unusual: it contains very few events for its long duration (Figure 21), and all six events have magnitudes between  $m_b = 4.8$  and 5.0 (Figure 22). The sequence of rupturing appears to migrate from east to west, over a distance of 10–20 km.

*Acknowledgments.* We thank Tom Jordan, Allan Rubin, Doug Toomey, and Doug Wiens for useful discussions and Fred Klein and Keith Sverdrup for helpful reviews. Inclusion of the May–June 1989 Reykjanes Ridge swarm in this paper would not have been possible without data provided by Bruce Presgrave of NEIS. We also

benefitted from information on other ongoing studies of this swarm provided by Robin Holcomb, John Delaney, and Clyde Nishimura. We thank Gretchen Zwart for analysis of uncertainties in the CMT solution for the largest event in this swarm. This research was supported by the National Science Foundation under grants EAR-8617967 and EAR-8817173 and by the National Aeronautics and Space Administration under grant NAG 5-814.

## REFERENCES

- Abdallah, A., V. Courtillot, M. Kasser, A.-Y. Le Dain, J.-C. Lépine, B. Robineau, J.-C. Ruegg, P. Tapponnier, and A. Taran-tola, Relevance of Afar seismicity and volcanism to the mechanics of accreting plate boundaries, *Nature*, 282, 17–23, 1979.
- Allard, P., H. Tazieff, and D. Dajlevic, Observations of seafloor spreading in Afar during the November 1978 fissure eruption, *Nature*, 279, 30–33, 1979.
- Atwater, T. M., Constraints from the FAMOUS area concerning the structure of the oceanic section, in *Deep Drilling Results in the Atlantic Ocean: Ocean Crust*, edited by M. Talwani, C. G. A. Harrison, and D. E. Hayes, pp. 33–42, AGU, Washington, D.C., 1979.
- Aumento, F., B. D. Loncarevic, and D. I. Ross, Hudson geotraverse: Geology of the Mid-Atlantic Ridge at 45°N, *Phil. Trans. R. Soc. London, Ser. A*, 268, 623–650, 1971.
- Ballard, R. D., and T. H. van Andel, Morphology and tectonics of the inner rift valley at lat 36°50'N on the Mid-Atlantic Ridge, *Geol. Soc. Am. Bull.*, 88, 507–530, 1977.
- Bergman, E. A., Intraplate earthquakes and the state of stress in oceanic lithosphere, *Tectonophysics*, 132, 1–35, 1986.
- Bergman, E. A., S. C. Solomon, W. S. D. Wilcock, and G. M. Purdy, On the seismic width of the transform fault zone of the Kane Fracture Zone (abstract), *Eos Trans. AGU*, 69, 476, 1988.
- Björnsson, A., K. Saemundsson, P. Einarsson, E. Tryggvason, and K. Grönvold, Current rifting episode in north Iceland, *Nature*, 266, 318–323, 1977.
- Brandsdóttir, B., and P. Einarsson, Seismic activity associated with the September 1977 deflation of Krafla volcano in north-eastern Iceland, *J. Volcanol. Geotherm. Res.*, 6, 197–212, 1979.
- Brocher, T. M., T-phases from an earthquake swarm on the Mid-Atlantic Ridge at 31.6°N, *Mar. Geophys. Res.*, 6, 39–49, 1983.
- Cann, J. R., New model for the structure of the ocean crust, *Nature*, 226, 928–930, 1970.
- Dziewonski, A. M., and D. L. Anderson, Travel times and station corrections for P waves at teleseismic distances, *J. Geophys. Res.*, 88, 3295–3314, 1983.
- Dziewonski, A. M., and F. Gilbert, The effect of small, aspherical perturbations on travel times and a re-examination of the corrections for ellipticity, *Geophys. J. R. Astron. Soc.*, 44, 7–17, 1976.
- Dziewonski, A. M., J. E. Franzen, and J. H. Woodhouse, Centroid-moment tensor solutions for January–March 1984, *Phys. Earth Planet. Inter.*, 34, 209–219, 1984.
- Dziewonski, A. M., J. E. Franzen, and J. H. Woodhouse, Centroid-moment tensor solutions for July–September 1984, *Phys. Earth Planet. Inter.*, 38, 203–213, 1985.
- Dziewonski, A. M., J. E. Franzen, and J. H. Woodhouse, Centroid-moment tensor solutions for July–September 1985, *Phys. Earth Planet. Inter.*, 42, 205–214, 1986.
- Dziewonski, A. M., G. Ekström, J. E. Franzen, and J. H. Woodhouse, Global seismicity of 1977: Centroid-moment tensor solutions for 471 earthquakes, *Phys. Earth Planet. Inter.*, 45, 11–36, 1987.
- Dziewonski, A. M., G. Ekström, J. E. Franzen, and J. H. Woodhouse, Global seismicity of 1982 and 1983: Additional centroid-moment tensor solutions for 553 earthquakes, *Phys. Earth Planet. Inter.*, 53, 17–45, 1988.
- Dziewonski, A. M., G. Ekström, J. H. Woodhouse, and G. Zwart, Centroid-moment tensor solutions for April–June 1989, *Phys. Earth Planet. Inter.*, in press, 1989.
- Einarsson, P., Seismicity and earthquake focal mechanisms along the mid-Atlantic plate boundary between Iceland and the Azores, *Tectonophysics*, 55, 127–153, 1979.
- Einarsson, P., and B. Brandsdóttir, Seismological evidence for lateral magma intrusion during the July 1978 deflation of the Krafla Volcano in NE-Iceland, *J. Geophys.*, 47, 160–165, 1980.
- Evernden, J., Precision of epicenters obtained by small numbers of world-wide stations, *Bull. Seismol. Soc. Am.*, 59, 1365–1398, 1969.
- Foulger, G. R., and R. E. Long, Anomalous focal mechanisms: Tensile crack formation on an accreting plate boundary, *Nature*, 310, 43–45, 1984.
- Francis, T. J. G., The seismicity of the Reykjanes Ridge, *Earth Planet. Sci. Lett.*, 18, 119–124, 1973.
- Francis, T. J. G., A new interpretation of the 1968 Fernandina Caldera collapse and its implications for the mid-ocean ridges, *Geophys. J. R. Astron. Soc.*, 39, 301–318, 1974.
- Francis, T. J. G., and I. T. Porter, A statistical study of Mid-Atlantic Ridge earthquakes, *Geophys. J. R. Astron. Soc.*, 24, 31–50, 1971.
- Francis, T. J. G., I. T. Porter, and R. C. Lilwall, Microearthquakes near the eastern end of St. Paul's Fracture Zone, *Geophys. J. R. Astron. Soc.*, 53, 201–217, 1978.
- Habermann, R. E., Consistency of teleseismic reporting since 1963, *Bull. Seismol. Soc. Am.*, 72, 93–111, 1982.
- Hall, J. M., Major problems regarding the magnetization of oceanic crustal layer 2, *J. Geophys. Res.*, 81, 4223–4230, 1976.
- Harrison, C. G. A., Tectonics of mid-ocean ridges, *Tectonophysics*, 22, 301–310, 1974.
- Harrison, C. G. A., and L. Stieltjes, Faulting within the median valley, *Tectonophysics*, 38, 137–144, 1977.
- Herrin, E. (Chairman), 1968 seismological tables for P phases, *Bull. Seismol. Soc. Am.*, 58, 1193–1241, 1968.
- Herrin, E., and J. Taggart, Source bias in epicenter determinations, *Bull. Seismol. Soc. Am.*, 58, 1791–1796, 1968.
- Herrin, E., W. Tucker, J. Taggart, D. W. Gordon, and J. L. Lobdell, Estimation of surface focus P travel times, *Bull. Seismol. Soc. Am.*, 58, 1273–1291, 1968.
- Hill, D. P., A model for earthquake swarms, *J. Geophys. Res.*, 82, 1347–1352, 1977.
- Huang, P. Y., and S. C. Solomon, Centroid depths and mechanisms of mid-ocean ridge earthquakes in the Indian Ocean, Gulf of Aden, and Red Sea, *J. Geophys. Res.*, 92, 1361–1382, 1987.
- Huang, P. Y., and S. C. Solomon, Centroid depths of mid-ocean ridge earthquakes: Dependence on spreading rate, *J. Geophys. Res.*, 93, 13,445–13,477, 1988.
- Huang, P. Y., S. C. Solomon, E. A. Bergman, and J. L. Nabelek, Focal depths and mechanisms of Mid-Atlantic Ridge earthquakes from body waveform inversion, *J. Geophys. Res.*, 91, 579–598, 1986.
- Jemsek, J. P., E. A. Bergman, J. L. Nabelek, and S. C. Solomon, Focal depths and mechanisms of large earthquakes on the Arctic mid-ocean ridge system, *J. Geophys. Res.*, 91, 13,993–14,005, 1986.
- Jordan, T. H., and K. A. Sverdrup, Teleseismic location techniques and their application to earthquake clusters in the south-central Pacific, *Bull. Seismol. Soc. Am.*, 71, 1105–1130, 1981.
- Julian, B. R., Evidence for dyke intrusion earthquake mechanisms near Long Valley caldera, California, *Nature*, 303, 323–325, 1983.
- Julian, B. R., and S. A. Sipkin, Earthquake processes in the Long Valley caldera area, California, *J. Geophys. Res.*, 90, 11,155–11,169, 1985.
- Karpin, T. L., and C. H. Thurber, The relationship between earthquake swarms and magma transport: Kilauea volcano, Hawaii, *Pure Appl. Geophys.*, 125, 971–991, 1987.
- Klein, F. W., Earthquakes at Loihi submarine volcano and the Hawaiian hot spot, *J. Geophys. Res.*, 87, 7719–7726, 1982.
- Klein, F. W., P. Einarsson, and M. Wyss, The Reykjanes Peninsula, Iceland, earthquake swarm of September 1972 and its tectonic significance, *J. Geophys. Res.*, 82, 865–888, 1977.
- Klein, F. W., R. Y. Koyanagi, J. S. Nakata, and W. R. Tanigawa, The seismicity of Kilauea's magma system, *U.S. Geol. Surv. Prof. Pap. 1350*, 1019–1186, 1987.
- Kong, L. S. L., E. A. Bergman, S. C. Solomon, and G. M. Purdy, Simultaneous characterization of Mid-Atlantic Ridge earthquakes by local and global seismic networks (abstract), *Eos Trans. AGU*, 69, 1440, 1988.
- Laughton, A. S., and D. Monahan, General Bathymetric Chart of the Oceans (GEBCO), 5th ed., sheet 5.04, Canad. Hydrogr. Serv., Ottawa, 1978.
- Lewis, B. T. R., The process of formation of ocean crust, *Science*, 220, 151–157, 1983.
- Lilwall, R. C., Seismicity of the oceanic rifts, in *Continental and*

- Oceanic Rifts, Geodyn. Ser.*, vol. 8, edited by G. Pálmason, pp. 63–80, AGU, Washington, D.C., 1982.
- Lilwall, R. C., T. J. G. Francis, and I. T. Porter, Ocean-bottom seismograph observations on the mid-Atlantic Ridge near 45°N—further results, *Geophys. J. R. Astron. Soc.*, 55, 255–262, 1978.
- Lin, J., and E. M. Parmentier, Mechanisms of lithospheric extension at mid-ocean ridges, *Geophys. J. R. Astron. Soc.*, 96, 1–22, 1989.
- Luyendyk, B. P., and K. C. Macdonald, Physiography and structure of the inner floor of the FAMOUS rift valley: Observations with a deep-towed instrument package, *Geol. Soc. Am. Bull.*, 88, 648–663, 1977.
- Macdonald, K. C., Near-bottom magnetic anomalies, asymmetric spreading, oblique spreading, and tectonics of the Mid-Atlantic Ridge near lat 37°N, *Geol. Soc. Am. Bull.*, 88, 541–555, 1977.
- Macdonald, K. C., Mid-ocean ridges: Fine scale tectonic, volcanic and hydrothermal processes within the plate boundary zone, *Ann. Rev. Earth Planet. Sci.*, 10, 155–190, 1982.
- Macdonald, K. C., The crest of the Mid-Atlantic Ridge: Models for crustal generation processes and tectonics, in *The Geology of North America, Volume M, The Western North Atlantic Region*, edited by P. R. Vogt and B. E. Tucholke, pp. 51–68, Geol. Soc. Am., Boulder, Colo., 1986.
- Macdonald, K. C., and T. M. Atwater, Evolution of rifted ocean ridges, *Earth Planet. Sci. Lett.*, 39, 319–327, 1978.
- Mogi, K., Earthquakes and fractures, *Tectonophysics*, 5, 35–55, 1967.
- Mohr, P. A., The Afar triple junction and sea-floor spreading, *J. Geophys. Res.*, 75, 7340–7352, 1970.
- Needham, H. D., P. Choukroune, J. L. Cheminee, X. Le Pichon, J. Francheteau, and P. Tapponnier, The accreting plate boundary: Ardoukôba Rift (northeast Africa) and the oceanic rift valley, *Earth Planet. Sci. Lett.*, 28, 439–453, 1976.
- Phillips, J. D., R. E. Needham, and R. M. Sheppard, Seismic ray tracing for relocating oceanic ridge earthquakes, *Lincoln Lab. Tech. Rep. ESD-TR-78-259*, 7–14, Mass. Inst. of Technol., Cambridge, 1979.
- Phipps Morgan, J., E. M. Parmentier, and J. Lin, Mechanisms for the origin of mid-ocean ridge axial topography: Implications for the thermal and mechanical structure of accreting plate boundaries, *J. Geophys. Res.*, 92, 12,823–12,836, 1987.
- Reichle, M. S., and I. Reid, Detailed study of earthquake swarms from the Gulf of California, *Bull. Seismol. Soc. Am.*, 67, 159–171, 1977.
- Rubin, A. M., and D. D. Pollard, Dike-induced faulting in rift zones of Iceland and Afar, *Geology*, 16, 413–417, 1988.
- Ruegg, J.-C., J.-C. Lépine, A. Tarantola, and M. Kasser, Geodetic measurements of rifting associated with a seismo-volcanic crisis in Afar, *Geophys. Res. Lett.*, 6, 817–820, 1979.
- Schouten, H., Klitgord, K. D., and J. A. Whitehead, Segmentation of mid-ocean ridges, *Nature*, 317, 225–229, 1985.
- Searle, R. C., and A. S. Laughton, Sonar studies of the Mid-Atlantic Ridge and Kurchatov Fracture Zone, *J. Geophys. Res.*, 82, 5313–5328, 1977.
- Searle, R. C., D. Monahan, and G. L. Johnson, General bathymetric chart of the oceans (GEBCO), 5th ed., sheet 5.08, Canad. Hydrogr. Serv., Ottawa, 1982.
- Shaw, H. R., The fracture mechanisms of magma transport from the mantle to the surface, in *Physics of Magmatic Processes*, edited by R. B. Hargraves, pp. 201–264, Princeton University Press, Princeton, N. J., 1980.
- Sigurdsson, O., Surface deformation of the Krafla fissure swarm in two rifting events, *J. Geophys.*, 47, 154–159, 1980.
- Solomon, S. C., P. Y. Huang, and L. Meinke, The seismic moment budget of slowly spreading ridges, *Nature*, 334, 58–61, 1988.
- Stakes, D., J. W. Shervais, and C. A. Hopson, The volcanic-tectonic cycle of the FAMOUS and AMAR valleys, Mid-Atlantic Ridge (36°47'N): Evidence from basalt glass and basalt phenocryst compositional variations for a steady-state magma chamber beneath the valley midsections, AMAR 3, *J. Geophys. Res.*, 89, 6995–7028, 1984.
- Sykes, L. R., Earthquake swarms and sea-floor spreading, *J. Geophys. Res.*, 75, 6598–6611, 1970.
- Tamsett, D., Median valley tectonics; air photographs of the Ghoubbet-Asal Rift, Afar, *Tectonophysics*, 131, 75–88, 1986.
- Tapponnier, P., and J. Francheteau, Necking of the lithosphere and the mechanics of slowly accreting plate boundaries, *J. Geophys. Res.*, 83, 3955–3970, 1978.
- Tatham, R. H., and J. M. Savino, Faulting mechanisms for two oceanic earthquake swarms, *J. Geophys. Res.*, 79, 2643–2652, 1974.
- Thatcher, W., and J. Brune, Seismic study of an oceanic ridge earthquake swarm in the Gulf of California, *Geophys. J. R. Astron. Soc.*, 22, 473–489, 1971.
- Toomey, D. R., S. C. Solomon, G. M. Purdy, and M. H. Murray, Microearthquakes beneath the median valley of the Mid-Atlantic Ridge near 23°N: Hypocenters and focal mechanisms, *J. Geophys. Res.*, 90, 5443–5458, 1985.
- Toomey, D. R., S. C. Solomon, and G. M. Purdy, Microearthquakes beneath the median valley of the Mid-Atlantic Ridge near 23°N: Tomography and tectonics, *J. Geophys. Res.*, 93, 9093–9112, 1988.
- Tréhu, A. M., J. L. Nábelek, and S. C. Solomon, Source characterization of two Reykjanes Ridge earthquakes: Surface waves and moment tensors; *P* waveforms and nonorthogonal nodal planes, *J. Geophys. Res.*, 86, 1701–1724, 1981.
- Tryggvason, E., Seismicity, earthquake swarms, and plate boundaries in the Iceland region, *Bull. Seismol. Soc. Am.*, 63, 1327–1348, 1973.
- Vogt, P. R., Asthenosphere motion recorded by the ocean floor south of Iceland, *Earth Planet. Sci. Lett.*, 13, 153–160, 1971.
- Vogt, P. R., and G. L. Johnson, Transform faults and longitudinal flow below the midoceanic ridge, *J. Geophys. Res.*, 80, 1399–1428, 1975.
- Ward, P. L., New interpretation of the geology of Iceland, *Geol. Soc. Am. Bull.*, 82, 2991–3012, 1971.
- Wendt, K., D. Möller, and B. Ritter, Geodetic measurements of surface deformations during the present rifting episode in NE Iceland, *J. Geophys. Res.*, 90, 10,163–10,172, 1985.
- Whitehead, J. A., Jr., H. J. B. Dick, and H. Schouten, A mechanism for magmatic accretion under spreading centers, *Nature*, 312, 146–148, 1984.

E. A. Bergman and S. C. Solomon, Building 54-512, Department of Earth, Atmospheric, and Planetary Sciences, Massachusetts Institute of Technology, Cambridge, MA 02139.

(Received May 31, 1989;  
revised November 6, 1989;  
accepted November 8, 1989.)